Reactive Oxygen Production and Scavenging in Marine Phytoplankton

BY

Naaman Omar

A thesis submitted to the

Department of Biology

Mount Allison University

In partial fulfillment of the requirements for the

Bachelor of Science degree with Honours

May 4th, 2020.

Table of Contents

Acknowledgements 4
Abstract 5
List of Tables 6
List of Figures 6
Introduction 7
Phytoplankton Overview 7
Glaucophytae 8
Viridiplantae 9
Rhodophyta 9
Photosynthesis in Phytoplankton 11
Reactive Oxygen Species 11
Types of ROS 12
ROS Production 13
Alternative oxidase and Plastid terminal oxidase 13
Nitric oxide synthase 14
Nitrate reductase & Sulfite oxidase 14
Glycolate oxidase 15
Xanthine oxidase and Aldehyde oxidase 15
ROS Scavenging 15
Superoxide dismutase 16
Ascorbate glutathione cycle 16
Peroxidases and Catalase 17
Peroxiredoxins 18
Black Queen Hypothesis 19
Significance and Hypotheses 20
Materials & Methods 21
Genes Analysed 21
Bioinformatic procedure 23
Data analysis 25
Results 26
Discussion 35
Genome vs. transcriptomic data 35

ROS Production and Scavenging genes increase with increasing genome size and cell diameter 35
Conclusions and Future Directions 38
Supplemental Data 39
Bibliography 57
Appendices 72
Appendix 1 72
Probes for ROS Production enzymes 72
Probes for ROS Scavenging enzymes 75
Appendix 2 79

Acknowledgements

I would like to thank Doulas A. Campbell for his guidance and support throughout the course of this project. I would also like to acknowledge Katherine Fleury for providing initial materials and methods, figure organization and her expertise on this project. I would also like to thank the various members of the Campbell lab for their support throughout this period, as well as Matt Betti and Melissa Rioux for teaching me R. This work was supported by the Canada Research Chair's funding. I would also like to thank I. Kaczmarska, my second reader for early comments & Mats Töpel for the *Skeletonema marinoi* genome. Some sequences were accessed from The Marine Microbial Eukaryotic Transcriptome Sequencing Project (MMETSP) supported by the Gordon and Betty Moore Foundation through a grant to the National Center for Genome Resources.

Abstract

Phytoplankton are unicellular photosynthetic microorganisms adapted to live in open water. They use reactive oxygen species (ROS) for cell to cell signalling, although biotic or abiotically produced ROS can be harmful in higher concentrations and therefore phytoplankton must maintain ROS homeostasis. The Black Queen Hypothesis suggests that loss of function mutations carry on until the cost outweighs the benefit [1]. As it is harder for larger phytoplankton to get rid of ROS as it does not readily diffuse out of the cell, we investigated whether they would have more ROS detoxification genes, and fewer ROS producing genes. We indeed found a breakpoint at 3µm above which cells carry more genes encoding ROS scavenging. We could not determine whether there is an effect of cell size on the total genetic capacity for ROS production. The number of genes associated with ROS production and scavenging increased with larger genome size, although the slope was smaller than that of gene model size vs. genome size, indicating that less of the genome is allocated to ROS production and scavenging in larger genomes.

List of Tables

Table 1: ROS Production and Scavenging enzymes analyzed…….……22

Supplemental Table 1: Accession information, cell diameter, genome size and gene model count……...…39

Supplemental Table 2: ROS Production Gene Count per Taxon…….…….45

Supplemental Table 3: ROS Scavenging Gene Count per Taxon……...……..47

List of Figures

Figure 1: Evolution of phytoplankton……..……8

Figure 2: Formation of different types of ROS from molecular oxygen and structure of NO ….12

Figure 3: The Ascorbate glutathione cycle, and the breakdown mechanism of H_2O_2……...17

Figure 4: Catalytic and regulatory cycles of 2-Cys Peroxiredoxin……19

Figure 5: Schematic representation of the bioinformatic procedure used…….24

Figure 6: Comparison of genome size (in Mbp) with Diameter of a cell (in µm)…….26

Figure 7: Comparison of paired genomic vs. transcriptomic ROS detoxification gene counts from phytoplankton taxa…….27

Figure 8: Sum of Gene Models and ROS production gene count encoded within each taxon plotted vs. cell size…….28

Figure 9: Sum of Gene Models and ROS detoxification genes encoded within each taxon plotted vs. cell size…….29

Figure 10: Sum of Gene Models and ROS production gene count encoded within each taxon plotted vs. Genome size…….30

Figure 11: Sum of Gene Models and ROS scavenging gene count encoded within each taxon plotted vs. Genome size…….31

Figure 12: log10 (ROS Producing Gene Count +1) for each ROS scavenging enzyme functional group analysed vs. log10 (Median Cell Diameter, µm)…….32

Figure 13: log10 (ROS Scavenging Gene Count +1) for each ROS detoxification enzyme functional group analyzed vs. log10 (Median Cell Diameter, µm)……33

Introduction

Phytoplankton Overview

Phytoplankton are unicellular oxygenic photosynthetic microorganisms that are adapted to live partly or entirely in open water [2]. They are primary producers and are responsible for 45% of all primary production, at the lowest trophic level, making them of high importance [3–5]. Their biomass is approximately 1 to 2% of all global photosynthetic biomass, yet they take up 30 to 50 billion metric tonnes of carbon dioxide annually, another reason for their high global importance [6]. Evolutionarily, phytoplankton are not one distinct clade, but various supergroups within the eukaryote and bacteria domains [4]. The majority of phytoplankton within the bacterial domain, referred to as cyanobacteria, are unicellular picoplankton (1 to 3µm) of the *Prochlorococcus*, *Synechocystis*, *Synechococcus* and *Chroococcus* genera [7,8]. Approximately 1.5 billion years ago an endosymbiotic event took place, whereby a cyanobacterium was incorporated into a eukaryotic cell to form the heterotrophic ancestor to the Archaeplastidia represented by three modern day primary endosymbiotic algal groups, the Viridiplantae, Rhodophytes and Glaucophytes as seen in Figure 1 [9–11]

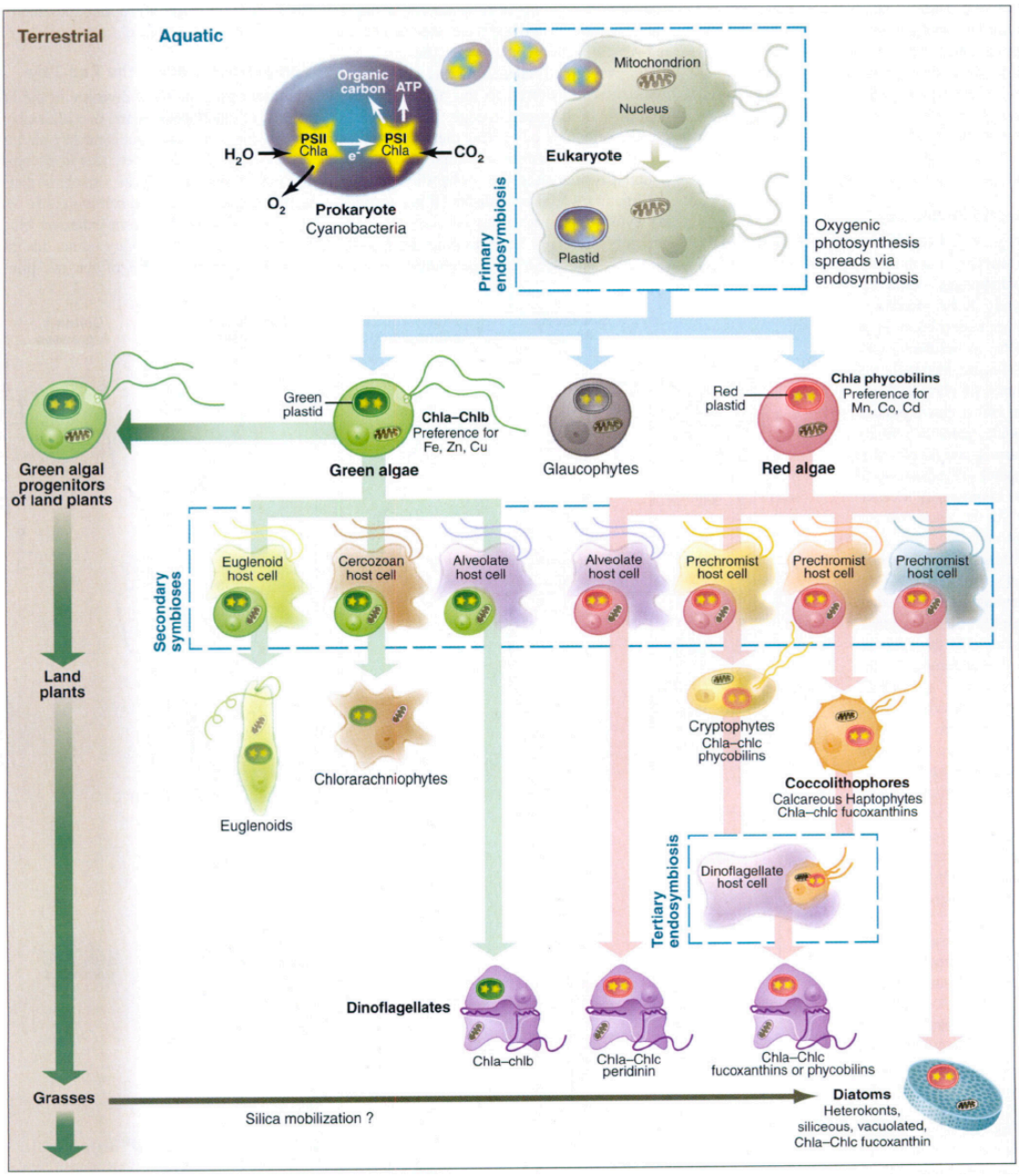

Figure 1: ***Evolution of phytoplankton****. This image visualizes the primary, secondary and tertiary endosymbiotic events behind the inheritance of plastids in Green algae, Glaucophytes and Red algae. Image derived from [9]*

Glaucophytae

The Glaucophytae are an archaeplastidial lineage distinguished by the presence of chlorophyll a and phycobilins, with cyanobacteria-like plastids surrounded by a peptidoglycan wall [12,13].

They have not been included in this study of marine phytoplankters as they are freshwater and terrestrial unicellular cells.

Viridiplantae

Viridiplantae consist of two main lineages; Chlorophyta and Streptophyta. The Chlorophytes include the majority of green algal species [10,14]. Chlorophytes are divided into a basal radiation of Prasinophyceae lineages and the 'core chlorophytes' which include the Chlorodendrophyceae and the Ulvophyceae, Trebouxiophyceae and Chlorophyceae, commonly referred to as the UTC [10]. Prasinophytes are an early diverging paraphyletic group of algae from 9 different lineages, which include the smallest living eukaryote, *Ostreococcus tauri* [15,16]. As prasinophytes are the earliest diverging lineages of the chlorophytes, they have had their genomes analysed in great detail, as they probably hold the key to the nature of the first viridiplantae [14]. Chlorodendrophyceae contains algae such as *Tetraselmis* and *Scherfferlia* previously characterized as Prasinophytes, but which have more recently been found to have more in common with the UTC group [10]. The core chlorophytes (UTC) are ecologically diverse. Ulvophyceae are mainly found in coastal regions, while Trebouxiophyceae and Chlorophyceae are found in freshwater and terrestrial environments, with some species in brackish and marine environments [10]. The Streptophyta includes the filamentous Charophytes, some freshwater algae and the land plant radiation. It is also worth noting that Streptophytes also include the Eustigmatophyceae algae, of which three genomes have been used for this study, and which are distinguishable from other algae because of their use of xanthophyll [17]. Secondary endosymbiosis involving the capture of a green alga by a non-photosynthetic protist resulted in the formation of the lineages of euglenids, chlorarachniophytes and a small group of dinoflagellates known as the green dinoflagellates, which are distinguished by having chlorophyll a and b [9,18].

Rhodophyta

Rhodophytes (red algae) lack chlorophyll b and c, but contain accessory pigments allophycocyanin, phycocyanin and phycoerythrin organized as phycobilisomes in unstacked thylakoids [19]. They are composed of two subphyla; Cyanidiophytina, which are extremophilic algae, and Rhodophytina which are primarily marine [19,20]. Only one primary rhodophyte was

used in this study (*Porphyridium purpureum*) as it is as yet the only marine phytoplanktonic mesophilic rhodophyte to have its genome sequenced. Unlike the green alga which contributed to three different known secondary endosymbiotic lineages, the rhodophytes only underwent one known endosymbiotic event, whereby a red alga was taken up by a Protista cell, which however then led to a diverse group of phytoplankton called the chromalveolates [18]. Lineages that acquired their secondary plastid in this manner include haptophytes, cryptomonads, diatoms and, directly or indirectly, the dinoflagellates [18].

Haptophytes are distinguishable by their flagella like structure used for the attachment to external surfaces and/or phagotrophic nutrition [21]. Multiple genomes from haptophyte phytoplankton have been sequenced and were used in this study.

Diatoms are best characterized by their silicate cell wall that evolved about 200 Mya [22]. They are ecologically diverse with many marine planktonic representatives, and are of various shapes and sizes (<2µm to >1mm) although the majority fall within the 10 to 100µm size range [23]. Diatoms contain chlorophyll a and c and comprise various classes; Coscinodiscophyceae – the centric diatoms, Mediophyceae – the bi- and multipolar centric diatoms, Flagilariophyceae – the pennate diatoms without a raphe and Bacillariophyceae – the pennate diatoms with a raphe [24–26].

Dinoflagellates are some of the most common marine microbial eukaryotes, with often massive genomes and unique molecular biology [27,28]. Dinoflagellates size ranges also vary with small dinoflagellates like those from the genus *Peridinium* being ~10µm, and large dinoflagellates like those from the genus *Ceratium* which can reach up to 400µm in length [190]. A few green dinoflagellates were formed as a result of an endosymbiotic event with a green alga was taken up. Most dinoflagellates are rather the result of secondary endosymbiosis of a rhodophyte or even tertiary endosymbiosis of a secondary rhodophyte endosymbiont [9]. Some dinoflagellate genomes have been sequenced and were used in this study.

Eukaryotic phytoplankton thus comprise diverse lineages that gained photosynthesis through primary, secondary or tertiary endosymbiosis (Figure 1) [2]. Eukaryotic phytoplankton span a large range of diameters, from the Prasinophyte *Ostreococcus tauri* (<1µm) to the diatom *Coscinodiscus wailesii* ranging up to 500µm [15,29]. Horizontal gene transfers of genetic

capacities and differential nutrient requirements also contribute to extensive variation across phytoplankton [30]. Studies predict that rising sea temperatures and the resulting stratification will favour the dominance of picophytoplankton with a reduction in diversity of larger species [31–33].

Photosynthesis in Phytoplankton

Photosynthesis can either be C_3 or C_4 whereby C_3 metabolism involves carbon fixation directly by the enzyme Rubisco, whereas C_4 metabolism uses PEP carboxylase for initial carbon fixation, followed by internal release of CO_2 for fixation by Rubisco [201]. Most phytoplankton were originally thought to undergo C_3 metabolism, although metabolic labelling and genome sequencing of the green algae, *Ulva prolifera,* and of the diatoms *Thalassiosira pseudonana* and *Thalassiosira weissflogii* reveal that they may also perform C_4 photosynthesis [199,200]. In the process, electrons are constantly moved from donor to acceptor, because of which, it is unsurprising that Reactive Oxygen Species are produced in abundance [202].

Reactive Oxygen Species

Reactive Oxygen Species (ROS) are reduced or activated forms of oxygen. ROS include free radicals – an oxygen atom containing one or more unpaired electrons such as hydroxyl radical ($^{\bullet}OH$) and the superoxide anion ($O_2^{\bullet-}$), or a non-radical oxygen such as hydrogen peroxide (H_2O_2) and singlet oxygen ($^1O_2$) [34–36]. ROS are a toxic but inevitable consequence of photosynthesis, but also hold other important functions in plant life, including signalling and defence [35,37,38]. Research suggests that ROS is involved in the pathway that establishes programmed cell death, and that ROS production is regulated by downstream products through negative feedback [38]. ROS plays an important role in inter-organellar signalling in plants, including part of the defence against pathogens [35,39,40]. This does not negate the fact that at higher concentrations or sustained exposures ROS has harmful effects on cells including the oxidation of proteins, enzyme inhibition and damage to DNA and RNA [35]. ROS levels within a cell are regulated by homeostasis as ROS levels below a minimum threshold sends the cell into a cytostatic state, as the cells can no longer maintain the useful functions requiring ROS, while ROS concentrations above the upper threshold drives the cell into a cytotoxic state where the cell is under oxidative stress and experiences the harmful effects of ROS [37,41].

Types of ROS

As seen in Figure 2A, in the ground state O_2 contains two parallel spin electrons in the π* 2p orbitals. Exciting these electrons results in one of two types of singlet oxygen; the delta state ($^1\Delta_g$ O_2) or the sigma state ($^1\Sigma_g$ O_2), both of which are more reactive than molecular O_2, although sigma state singlet oxygen is far more reactive as there are two anti-spin orbitals in the π* 2p orbitals [42,43].

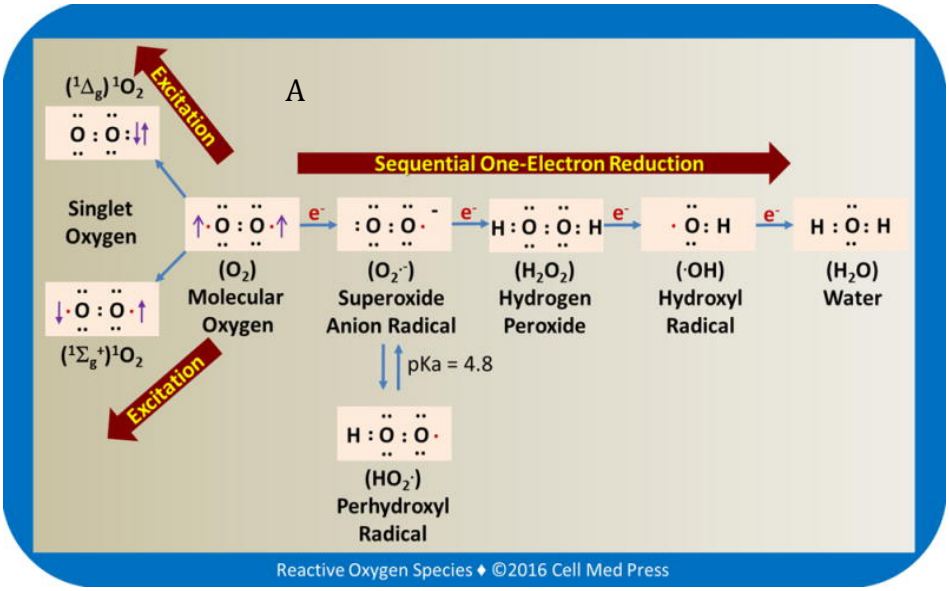

B

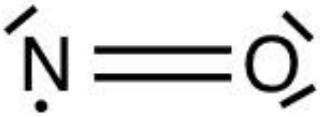

Figure 2: ***Formation of different types of ROS from molecular oxygen and structure of NO*** *[43].* ***2A****: Adding a single electron to molecular oxygen on the other hand reduces oxygen, changing it from a di-radical to a mono-radical, forming superoxide ($O_2^{\bullet-}$). Further reduction of the superoxide radical results in the formation of Hydrogen peroxide (H_2O_2). H_2O_2 can be reduced further to form the hydroxyl radical (•OH), which is further reduced to form water [42,43].* ***2B:*** *Nitric oxide is a radical compound with the unpaired electron located on the nitrogen.*

Superoxide ($O_2^{\bullet-}$) can be made by the addition of an electron to molecular oxygen. Subsequent addition of an electron and two protons results in the formation of hydrogen peroxide, whereas the addition of a proton to superoxide can result in the formation of perhydroxyl radical ($HO_2^{\bullet}$) at low pH. Further addition of an electron to H_2O_2 results in the formation of the hydroxyl radical (•OH). Lastly, the hydroxyl radical can be reduced down into H_2O by the addition of an electron and 2 protons (Figure 2A) [43,44]. Due to their radical nature $O_2^{\bullet-}$, $HO_2^{\bullet}$ and •OH tend to be more reactive than H_2O_2 [44]. As a result, H_2O_2 is able to penetrate across the cell membrane without

necessarily causing lipid damage, whereas $O_2^{\bullet-}$ cannot, and so, most $O_2^{\bullet-}$ produced from metabolism must be dealt with intracellularly [45]. Nitric oxide (NO) is a type of ROS that is also considered a Reactive Nitrogen Species (RNS). It is capable of permeating through the cell membrane due to its small, hydrophobic and neutral nature (Figure 2B) [196]. It is an important signalling molecule in marine microalgae responsible for mediating various population-level interactions [46–48].

ROS Production

ROS can be generated both enzymatically and non-enzymatically. Non-enzymatically, some molecules including glyceraldehyde, $FADH_2$, L-DOPA and oxidize in the presence of O_2 to form $O_2^{\bullet-}$ [42]. ROS also becomes more abundant when PSI function is compromised [74] thereby limiting the photochemical withdrawal of electrons from reduced electron carriers in the intersystem electron transport chain. Studies also suggest that mitochondria, specifically Complex II of the electron transport chain produces significant amounts of ROS, which allows it to act as a signalling organelle by contributing to gene expression through the production of NO and $O_2^{\bullet-}$ [75–77].

Photosystem II (PSII) is also a major contributor of ROS, as it is able to produce $^1O_2$ and H_2O_2 [78]. Mechanisms of $^1O_2$ formation by PSII include singlet oxygen produced from excitation transfer from excited pigments, particularly under high light, whereas hydrogen peroxide is formed directly from one-electron leakages, as for example from the water splitting complex of PSII [203].

Enzymatically peroxidases can produce ROS in the absence of their usual substrates, but in the presence of iron [79]. Specific enzymatic reactions involved in the production of ROS include:

Alternative oxidase and Plastid terminal oxidase

Mitochondrial alternative oxidase is an important enzyme involved in the mitochondrial electron transport chain [75] and acts like a buffer, by transferring extra electrons from the mitochondrial electron transport chain to oxygen [80] without direct coupling to accumulation of a trans-membrane proton gradient. One study found that knockdown mutations of mitochondrial AOX in the marine diatom *Phaeodactylum tricornutum* resulted in significantly lower photosynthetic

rates, and increased oxidation of the chloroplast, which suggests that AOX is crucial for cross-talk between the mitochondria and the chloroplast, although the exact mechanisms behind this crosstalk are not understood [81,82]. Lastly, while the mechanisms are not well understood, AOX is believed to carry out a role in the production/regulation of various ROS species, especially NO [83].

Plastid terminal oxidase (PTOX) on the other hand, is thought to be the plastidial ortholog of mitochondrial alternative oxidase and is attached to the thylakoid membrane [84, 191]. It is believed to have originally evolved from an alternative oxidase and is present in eukaryotes as a result of endosymbiosis of the cyanobacterium that became the plastid [193]. PTOX is also known to act as an anti-oxidant as well as a pro-oxidant based on the quinol concentration of the cell, and that the reactive oxygen species are produced as part of a side reaction [191,192].

Nitric oxide synthase

Nitric oxide synthase (NOS) codes for the production of Nitric Oxide (NO). NOS is typically found throughout the animal kingdom and some algal species, but not necessarily in higher plants, which suggests that the enzyme was lost during plant evolution [46]. In a previous study that searched transcriptomes for NOS-like sequences, the study found NOS in 15 of 265 algal species, although no correlation could be found between the 15 algal species [85,86].

Nitrate reductase & Sulfite oxidase

Nitrate reductase mediated formation of ROS is one of the better understood mechanisms and involves an initial conversion of nitrate to nitrite [86]. Another enzyme known as Nitric-Oxide - Forming Nitrite Reductase (NOFNiR) then synthesizes NO from nitrite through a series of complex molybdenum dependent reactions [46]. It is worth noting however that this is not the primary role of nitrate reductase, which is involved in various other cellular processes including nitrogen uptake [86]. Sulfite oxidase (SulOx) is also a fairly unexplored enzyme, although is known to produce H_2O_2 by oxidizing a molecule of sulfite using H_2O (Equation 1) [87,194].

$$SO_3^{2-} + O_2 + H_2O = SO_4^{2-} + H_2O_2 \qquad (1)$$

Glycolate oxidase

Glycolate oxidase (GOX) and glycolate dehydrogenase are two isoforms the same enzyme, of which glycolate dehydrogenase is commonly found in cyanobacteria [88]. GOX converts glycolate and O_2 into glyoxylate and H_2O_2 and is found in the peroxisome of the cell (Equation 2) [195].

$$a\ (S) - 2 - hydroxy\ carbolate + \ O_2 = a\ 2 - oxo\ carboxylate + \ H_2O_2 \qquad (2)$$

Xanthine oxidase and Aldehyde oxidase

Xanthine oxidase is an enzyme in the molybdenum hydrolase family that breaks down hypoxanthine into xanthine and in the process can produce $O_2^{\bullet-}$ or H_2O_2 [89–91]. Xanthine oxidase has also been shown to reduce nitrite into nitric oxide but only in oxygen lacking conditions (Equation 3) [90, 197].

$$Xanthine + H_2O + O_2 = urate + \ H_2O_2 \qquad (3)$$

Another enzyme, Aldehyde Oxidase is evolutionarily related to xanthine oxidase in that it is also a molybdenum hydrolase family enzyme, but one without well understood functions, except for the fact that it produces $O_2^{\bullet-}$ or H_2O_2 (Equation 4) [92, 198].

$$an\ aldehyde + \ H_2O + \ O_2 \rightarrow a\ carboxylate + \ H_2O_2 \qquad (4)$$

ROS Scavenging

In order to maintain equilibrium, ROS concentrations within the cell are lowered using a series of non-enzymatic and enzymatic reactions. Non-enzymatic reactions include those of tocopherols which undergo various redox reactions with different ROS species, in order to scavenge them, or carotenoids which have the ability to quench $^1O_2$ at high rates [49,50]. Enzymatic reactions to scavenge ROS include those catalysed by superoxide dismutase, peroxidases and catalase.

Superoxide dismutase

Superoxide dismutase (SOD) is involved in the catalytic breakdown of superoxide into hydrogen peroxide (Equation 5), using a metal co-factor [51].

$$2O_2^{\bullet -} + 2H^+ \rightarrow H_2O_2 + O_2 \qquad (5)$$

The metal co-factor used to facilitate this process can be Fe, Mn, Cu/Zn or Ni [52] depending upon the isoform of SOD. Fe-SODs are primarily found in the chloroplast, Mn-SODs in the mitochondria and Cu/Zn-SODs in the chloroplast and cytosol [53]. Fe-SODs and Mn-SODs are homologous and are believed to have evolved in early primitive life forms, while CuZn-SODs is primarily found in eukaryotes, and Ni-SODs in bacteria and algae [54]. Superoxide dismutases undergo negative inhibition by H_2O_2 [55], and so maintaining SOD activity requires scavenging of H_2O_2.

Ascorbate glutathione cycle

The Ascorbate-glutathione cycle, also known as the Halliwell-Asada cycle, plays an important role in ROS homeostasis through a series of enzymes connecting reductions of ascorbate, glutathione and NADPH [57]. The first step involves the reduction of H_2O_2 by ascorbate peroxidase (APX) at the expense of ascorbate (AsA), to yield monodehydroascorbate (MDHA) and H_2O (AsA) [57] (Figure 3). Monodehydroascorbate reductase (MDHAR) can then reduce MDHA back to AsA by transferring electrons from NADPH which is oxidized to NADP [58]. Alternately, two MDHA can non-enzymatically dismutate to a reduced AsA and an oxidized Didehydroascorbate (DHA). DHA, if formed, is then reduced back to AsA through the action of dehydroascorbate reductase (DHAR), which requires glutathione GSH as an electron donor, thus producing oxidized glutathione (GSSG) [59]. Glutathione Reductase then uses NADPH to reduce GSSG back to GSH using NADPH as a reducing agent [57], which allows it to be re-used for subsequent cycles (Figure 3).

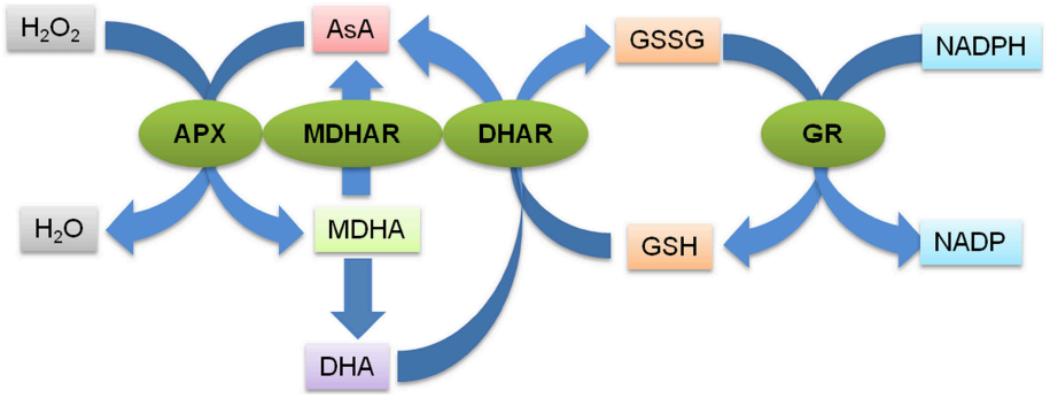

Figure 3: ***The Ascorbate glutathione cycle, and the breakdown mechanism of H_2O_2.*** *The green circles indicate the various enzymes in the cycle, and the blue arrows are the steps in the pathway. Abbreviations are as follows - APX, Ascorbate peroxidase; AsA, Ascorbic acid; MDHAR, Monodehydroascorbate reductase; MDHA, Monodehydroascorbate; DHA, Dehydroascorbate; DHAR, Dehydroascorbate reductase; GSSG, oxidized glutathione dimer; GSH, Glutathione; GR, Glutathione reductase.*

Peroxidases and Catalase

The three main enzymes involved in the catalysis of H_2O_2 are Ascorbate peroxidase (APX), Glutathione peroxidase (GPX), and Catalase (CAT), and of which APX is said to have the highest affinity for H_2O_2 [60,61].

Peroxidases follow the peroxidatic pathway (Equation 6), using an electron donor

$$H_2O_2 + 2AH_2 \rightarrow 2H_2O + 2AH \qquad (6)$$

Glutathione peroxidase breaks down H_2O_2 by directly using GSH as the reducing agent (AH_2) and produces GSSG (AH) and H_2O [62]. GR thereby bypasses the ascorbate peroxidase cycle. GPX and GR maintain the GSH/GSSG ratio [66].

Catalases decompose two H_2O_2 molecules and break them down into H_2O and O_2 (Equation 7) through a dismutation reaction without a requirement for metabolic reductant. Catalase is primarily found in the peroxisomes, but small amounts can also be found in the mitochondria, chloroplast and endoplasmic reticulum [62]. Most catalases are haem based, although pseudo-catalases, which are non-haem based use alternatives such as manganese [63]. Catalase activity can also be inhibited by the accumulation of superoxide [64,65].

$$2H_2O_2 \rightarrow 2H_2O + O_2 \qquad (7)$$

Catalase peroxidase (Katg), also responsible for the breakdown of H_2O_2, is primarily found in microbes and shares high homology with Cytochrome C Peroxidase (CCP) [67]. Although Katg is mainly found in bacteria, it is also found in some eukaryotes, which is attributed to probable horizontal transfer [68]. Interestingly, Katg is unique, in the sense that it can catalyse both the catalase pathway (Equation 7), as well as the peroxidatic pathway (Equation 6), although the peroxidatic pathway is more dominant at lower concentrations of H_2O_2 [68].

CCP like Katg and APX are class I peroxidases and follow the peroxidatic pathway to break down H_2O_2 by oxidizing Cytochrome C, to produce H_2O. In the process, CCP is regenerated [69,70]. Interestingly, phylogenetic analyses reveal that eukaryotic CCPs are more closely related to other peroxidases, including Katg, than to prokaryotic CCPs [71].

Peroxiredoxins

Peroxiredoxins are the most important and diverse family of peroxide and peroxynitrate scavenging enzymes [72]. They are highly conserved omnipresent group of peroxidases that interestingly do not contain any redox cofactors, including heme, metal ions and flavin [72,73]. There are six evolutionarily distinct subfamilies in nature that vary based on the location of the revolving cysteine and oligomer state; Prx1, Prx5, Prx6, Tpx, PrxQ and AhpE [72]. They are frequently found at high levels and can rapidly clear peroxides through either the catalytic cycle or redox regulation, the latter is more common in higher concentrations of peroxide (Figure 2) [72].

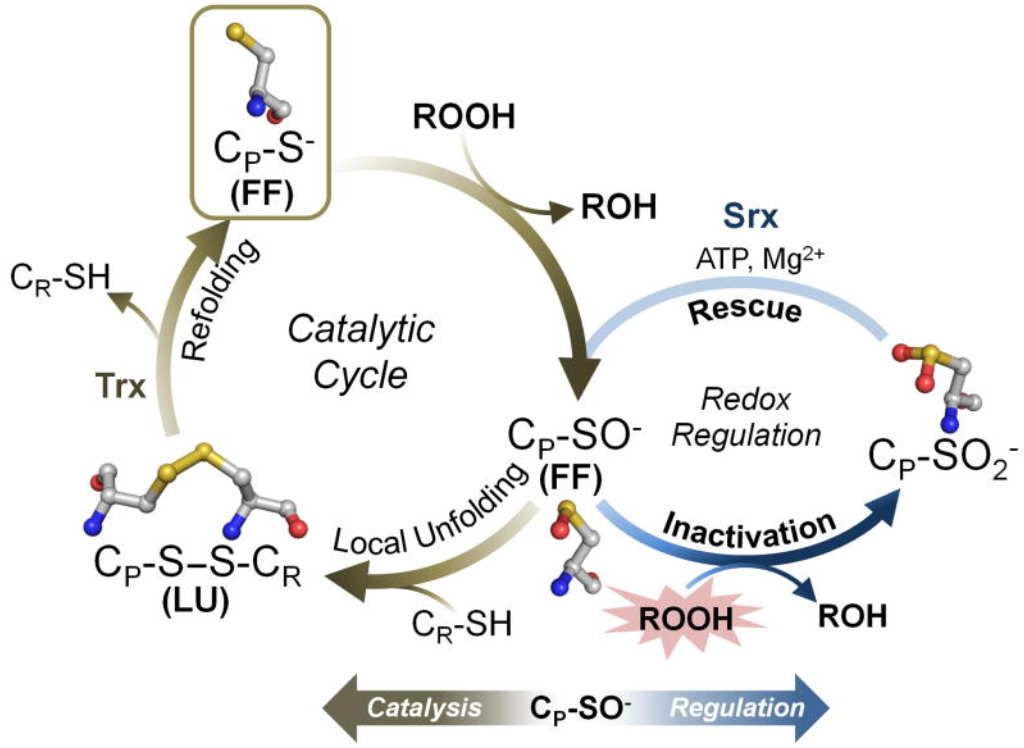

Figure 4: ***Catalytic and regulatory cycles of 2-Cys Peroxiredoxin [72].*** *The regulatory cycle seen in blue, a predominantly eukaryotic process for peroxide breakdown, is primarily used in cases where peroxide levels are high. The catalytic cycle seen in brown uses conformational change in the enzyme to break down peroxides.*

Black Queen Hypothesis

The Black Queen Hypothesis (BQH) is a theory that suggests that loss of function mutations can be selected in organisms in certain conditions, provided the entire community does not lose the function [1]. A loss of function mutation occurs as a result of gene loss during genome reduction and leaves the individual dependent on community members retaining the function [93]. H_2O_2 detoxification loss is a good example, in that *Prochlorococcus*, which lacks the gene encoding Katg, may require less iron than its ancestor which carried a gene encoding Katg using an iron cofactor, giving a potential benefit of losing Katg expression in regions with low iron. As long as other members in the community continue to detoxify H_2O_2 preventing a build-up, the *Prochlorococcus* will have increased its fitness. This can only occur where the benefits of loss outweigh the costs.

Significance and Hypotheses

In smaller cells, ROS is able to diffuse out more readily compared to larger cells. Therefore, small phytoplankton cells would not suffer detriment by losing a gene that codes for the production of an enzyme that scavenges ROS, whereas as a larger cell would suffer detriment. We therefore hypothesize that small cells undergo more loss of function mutations of ROS scavenging genes compared to larger cells, which we predict will show retention and expansion of gene families encoding ROs detoxification. At the same time, as ROS does not readily diffuse out of large cells, we hypothesize that large cells undergo more loss of function mutations in genes encoding ROS production, as they do not need to replenish the ROS that diffuses out in order to maintain the basal ROS level. Therefore, ROS scavenging and production genes were both analysed as part of this study of the capacities for ROS metabolism across size and taxonomic ranges of phytoplankters.

Materials & Methods

Genes Analysed

Genes that code for the production of an enzyme that either produces or scavenges ROS are mentioned in Table 1. ROS scavenging gene counts from green algae and diatoms were earlier analyzed by Kat Fleury as part of her thesis [94] using the same procedures, and were included in this wider study.

Table 1: ***ROS Production and Scavenging enzymes analyzed***

Enzyme Name	**Abbreviation**	**EC Number**	**Production/ Scavenging**
Superoxide Dismutase (Fe, Mn, Cu/Zn, Ni)	Fe-SOD, Mn-SOD, Cu/Zn-SOD, Ni-SOD	1.15.1.1	Scavenging
Glutathione reductase	GR	1.6.4.2	Scavenging
Monodehydroascorbate reductase	MDHAR	1.6.5.4	Scavenging
Dehydroascorbate reductase	DHAR	1.6.5.1	Scavenging
Ascorbate peroxidase	APX	1.11.1.11	Scavenging
Catalase peroxidase	Katg	1.11.1.21	Scavenging
Glutathione peroxidase	GPx	1.6.4.2	Scavenging
Cytochrome C peroxidase	CCP	1.11.1.5	Scavenging
Peroxiredoxin Q, Typical-2-Cys-Peroxiredoxin, Atypical 2-Cys-Peroxiredoxin, One-Cys-Peroxiredoxin	Prx Q, Typ2CysPrx, Atyp2CysPrx, OneCysPrx	1.11.1.15	Scavenging
Catalase	CAT	1.11.1.6	Scavenging
Alternative oxidase, Plastid terminal oxidase	AOX, PTOX	1.10.3.11	Production
Nitric oxide synthase	NOS	1.14.13.39	Production
Nitrate reductase	NR	1.7.1.1, 1.7.1.2, 1.7.1.3	Production
Glycolate oxidase	GlyOx	1.1.3.15	Production
Xanthine oxidase and aldehyde oxidase	XaAlOx	1.17.3.2, 1.2.3.1	Production
Sulfite oxidase	SulOx	1.8.3.1	Production

Bioinformatic procedure

The bioinformatic procedure was developed by Katherine Fleury as part of her thesis [94] with guidance from Dr. Marek Elias, University of Ostrava, Czech Republic. Probe sequences for gene families of interest were downloaded from the KEGG database [95–97] (https://www.genome.jp/kegg/) and compiled into a text file.

Genomic and/or transcriptomic data was obtained for marine oxygenic phytoplankton from Chrysophyte, Cryptophyte, diatom, Dinoflagellate, Eustigmatophyte, green algal, Haptophyte, Pelagophyte, *Prochlorococcus*, red algal and *Synechococcus* lineages. Genomic and transcriptomic data were downloaded from the Joint Genome Institute (JGI), pico-PLAZA, National Center for Biotechnology Information (NCBI), the Marine Microbial Eukaryotic Transcriptome Sequencing Project (MMETSP), the European Nucleotide Archive (ENA), iMicrobe, the 1000 Plants project (1KP), Greenhouse and Reef Genomics in .txt, .fasta or .fa formats[98–106]. Genomic and transcriptomic data were both used in this study as a means of increasing the range of cell size and taxonomic coverage as at the time of this study, as some species had their transcriptomes sequenced but not their genome. Due to the difference in information between a genome and a transcriptome, for some organisms, we analysed both the genome and the corresponding transcriptome to understand whether the two data types generated different patterns.

Freshwater and extremophile species were filtered out because the ROS environments in fresh water or extreme environments differ significantly from seawater. Information including the longitude and latitude that the cell was isolated from, the cell diameter range and motility were collected from the literature or culture collection documentation, and have been summarized in Supplemental Table 1. In cases where there was a range in the reported cell diameter for a taxon, the diameter used in the analysis was the average between the largest and smallest reported diameter. We did not pursue more sophisticated analyses of different cell shapes across taxa, which is a subject for future study. Motility was inferred by the presence or absence of a flagella.

Probe sequence homologs were searched for within genomes and transcriptomes using command line Basic Local Alignment Search Tool (BLAST+) version 2.9.0+. The procedure involves two parts, making a database, which allows the computer to read the genome or transcriptome file,

and then searching the file for the sequences of interest, specifically those matching a probe sequence with an e-value of less than 0.50. For a genome, these two parts would be run using the following code:

./makeblastdb -in protein_file_name.txt -dbtype prot

./blastp -query sequencefile.txt -db protein_file_name.txt -out output.txt -evalue 0.50.

For a transcriptome, these two parts would be run using the following code:

./makeblastdb -in protein_file_name.txt -dbtype nucl

./tblastn -query sequencefile.txt -db protein_file_name.txt -out output.txt -evalue 0.50.

Output sequences were then confirmed by running them as a query sequence on NCBI BLAST [107] to determine if they indeed match to members of the expected gene family when used as probes. Sequences that were confirmed were entered as raw data (Supplemental table 2 & 3). Figure 5 presents a summary of this procedure.

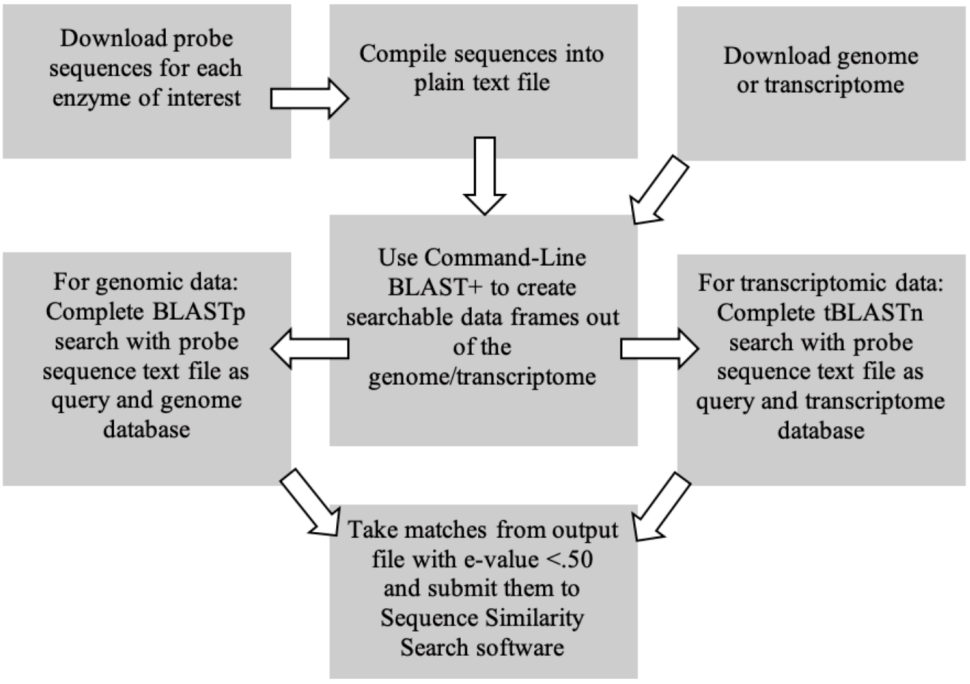

Figure 5: ***Schematic representation of the bioinformatic procedure used.*** *Image produced by Katherine Fleury [94].*

Data analysis

Raw data was analysed using R (RStudio Team, 2019) and analysed and plotted using the ‘tidyverse’ [108], ‘ggplot2’ [109], ‘cowplot’ [110], ‘broom’ [111],‘magrittr’ [112], ‘dplyr’ [113], ‘ggpubr’ [114], ‘glue’ [115], ‘kableExtra’ [116], ‘chngpt’ [117], ‘rcompanion’ [118], ‘corrplot’ [119], ‘ggfortify’ [120,121], ‘gmodels’ [122], ‘stats’ [189] and ‘smatr’ [123] packages. Citations were managed using the Zotero (www.zotero.org) open access reference manager connected to RStudio using the ‘citr’ [124] package, with output generated using the ‘knitr’ [125–127] and ‘bookdown’ [128] packages.

Results

We initially compared the diameters of various cells with the size of their genome. In general, larger cells had larger genomes, and prokaryotes (*Prochlorococcus* and *Synechococcus*) had smaller genomes than eukaryotes of similar size (Green Prasinophytes) (Figure 6). Cell and genome sizes also varied systematically with taxonomic grouping, as for example the large cells and genomes of all analysed Dinoflagellates. These taxonomic co-variances were coded using symbol colour in figures but were not pursued analytically and are the subject for future study.

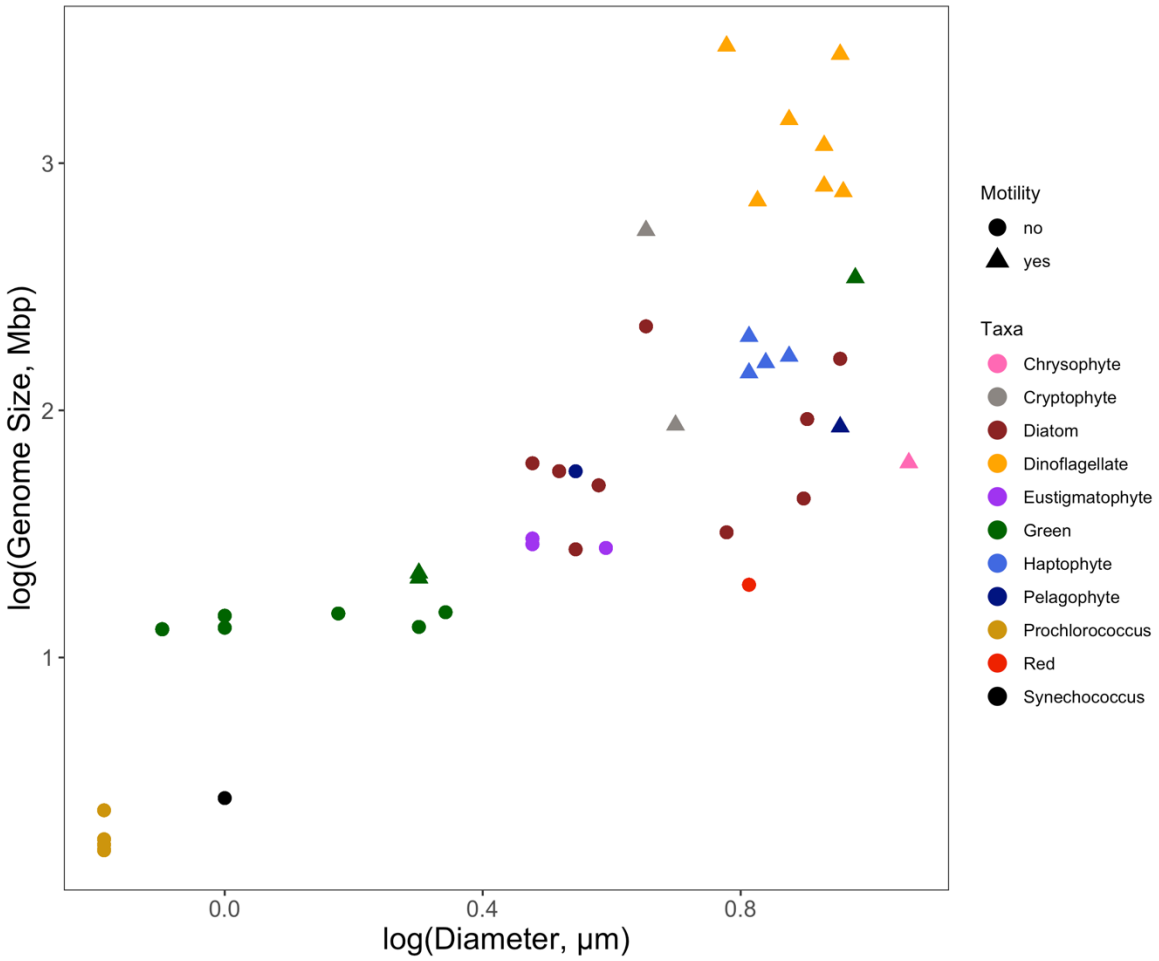

Figure 6: ***Comparison of genome size (in Mbp) with Diameter of a cell (in µm).*** *Colour corresponds to the taxon lineage, whereas shape indicates the motility of the species, which was indicated by the presence/absence of a flagella. Transcriptomic data was filtered out. Citations for data sources in Supplemental Data Table 1.*

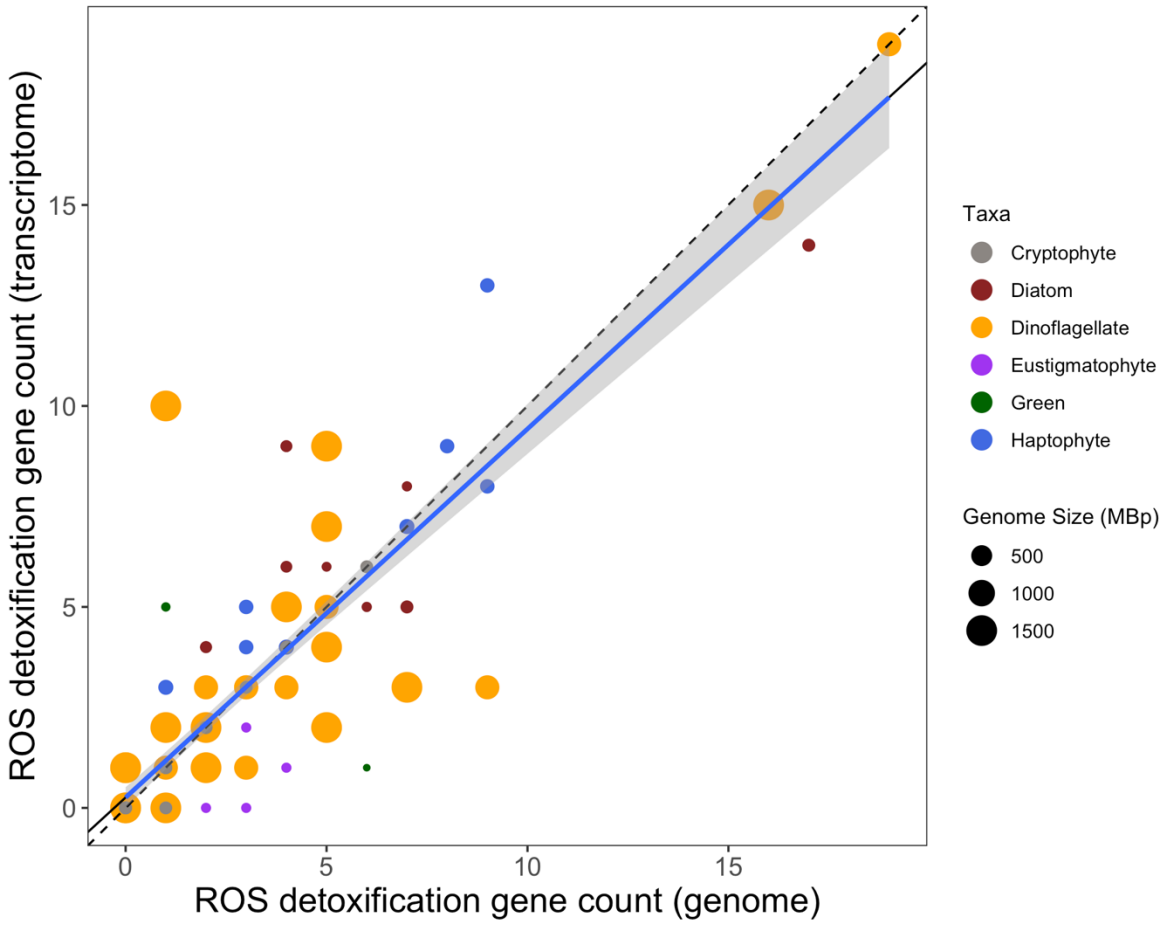

Figure 7: ***Comparison of paired transcriptomic vs. genomic ROS detoxification gene counts from phytoplankton taxa.*** *Symbol colour corresponds to the taxon lineage, whereas symbol size is proportional to the size of the genome in Mbp. Dashed line shows a 1:1 line, whereas the solid blue line shows the linear regression with the shaded region referring to ± 95% Confidence Intervals. Citations for data sources in Supplemental Data Table 1.*

We compared 12 paired genomes and transcriptomes drawn from the same organism, covering 6 different taxonomic lineages. Figure 7 is a comparison of these paried ROS detoxification gene counts, showing a slope of 0.92 ± 0.08 and an intercept of 0.26 ± 0.128. Upon comparing the linear model with the 1:1 line using an offset [189], we concluded that there is no statistically significant difference ($p = 0.02$) in gene counts for ROS detoxification derived from genomes vs. the paired transcriptome from the same taxa. Therefore in subsequent analyses we pooled transcriptomic and genomic data, although we retained coding of the data source using the symbol types on figures.

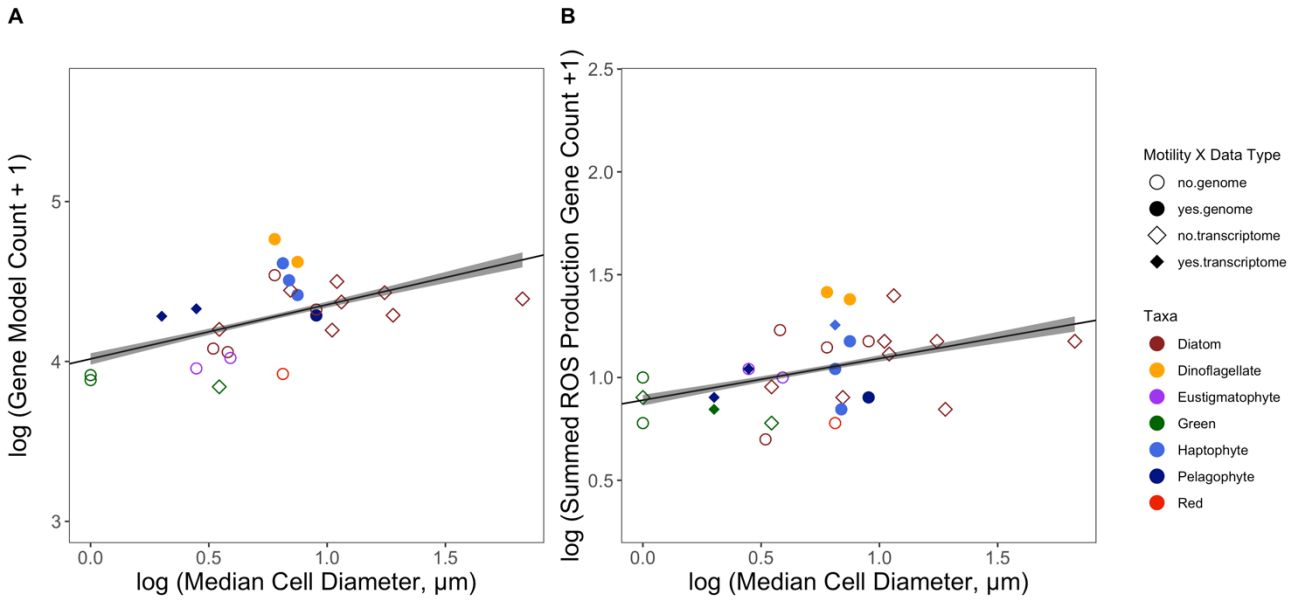

Figure 8: **Sum of Gene Models and ROS production gene count encoded within each taxon plotted vs. cell size.** ***A:*** *log10 (Gene Model Count) vs. log10 (Median Cell Diameter (µm)) for those taxa with gene model count data available. Gene model counts for transcriptomic data were assumed equal to the total number of transcribed products detected.* ***B:*** *log10 (Sum of ROS production genes) vs. log10 (Median Cell Diameter (µm)) for each taxon. Regression fitted to all data (solid line) ± 95% Confidence Intervals (grey band). Symbol colour corresponds to taxon lineages. Filled symbols indicate species that are motile. Motility was determined by the presence/absence of a flagella. Circular symbols represent genomic data and diamond symbols represent transcriptomic data. Citations for data sources in Supplemental Data Table 1.*

In Figure 8A, we plotted the gene model count vs. the median cell diameter and found a positive trend; the slope of log10 Gene model count vs. log10 Median Cell Diameter was 0.34 ± 0.08, hence, as expected, larger cells have more genes. We then (Fig. 8B) plotted the total number of genes that produced ROS vs. log10 Median Cell Diameter which also had a positive trend of 0.20 ± 0.06 indicating that larger cells have more genes that produce more ROS, but that ROS production genes increase less with cell size than does the wider count of gene models.

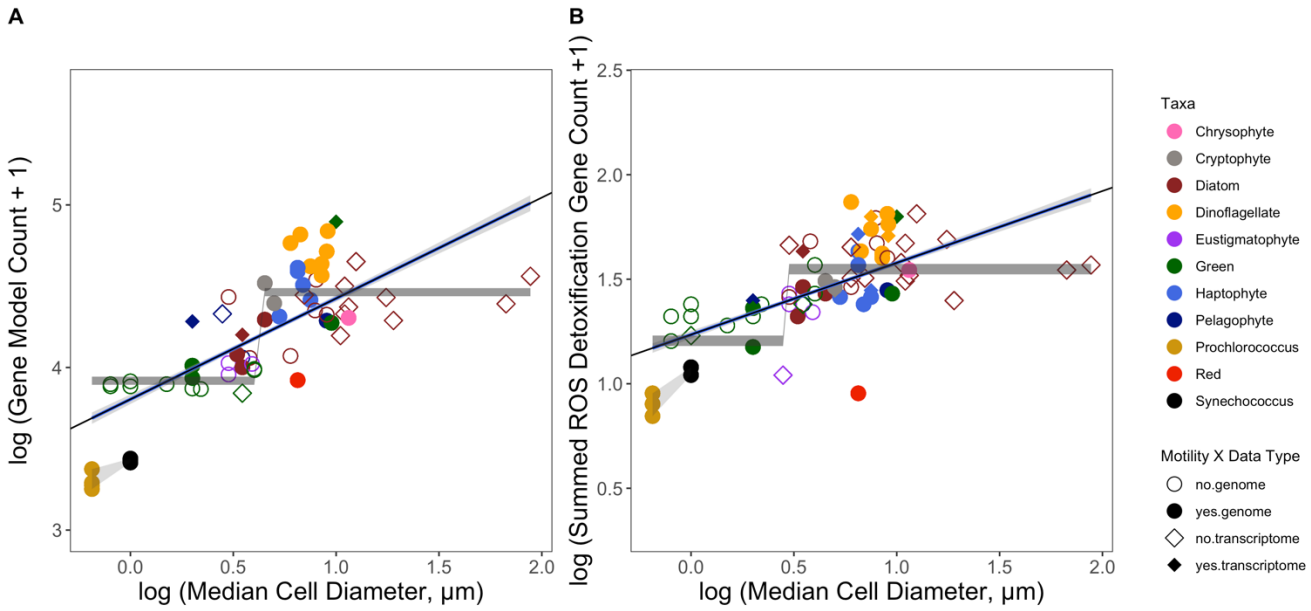

Figure 9: ***Sum of Gene Models and ROS detoxification genes encoded within each taxon plotted vs. cell size. A:*** *log10 (Gene Model Count) vs. log10 (Median Cell Diameter (µm)) for those taxa with gene model count data available. Gene model counts for transcriptomic data were assumed equal to the total number of transcribed products detected,* ***B:*** *log10 (Sum of ROS detoxification genes) vs. log10 (Median Cell Diameter (µm)) for each taxon. Regression fitted to all data (solid line) with stepped threshold (grey band), Grey area outlines prokaryotic data excluded from regressions but presented for comparison. Symbol colour corresponds to taxon lineages. Filled symbols indicate species that are motile. Motility was determined by the presence/absence of a flagella. Circular symbols represent genomic data and diamond symbols represent transcriptomic data. Citations for data sources in Supplemental Data Table 1.*

Figure 9 compares the total gene model count and the total number of genes that scavenge ROS to the cell diameter using two analyses; a linear model and a breakpoint analysis using the 'chngpt' package [117]. Figure 9A compares total genes vs. cell diameter, the linear model predicts a slope of 0.73 ± 0.22, whereas the breakpoint predicts a step change at 4.5µm ($p = 3.97E-14$), whereas, in Figure 9B, the linear model predicts a slope of 0.34 ± 0.02, whereas a breakpoint analysis predicts a step change at 3.0µm ($p = 6.23E-21$). It is also worth noting that Figure 9 omits transcriptomic data sets for which the total number of transcripts counted was not obtained.

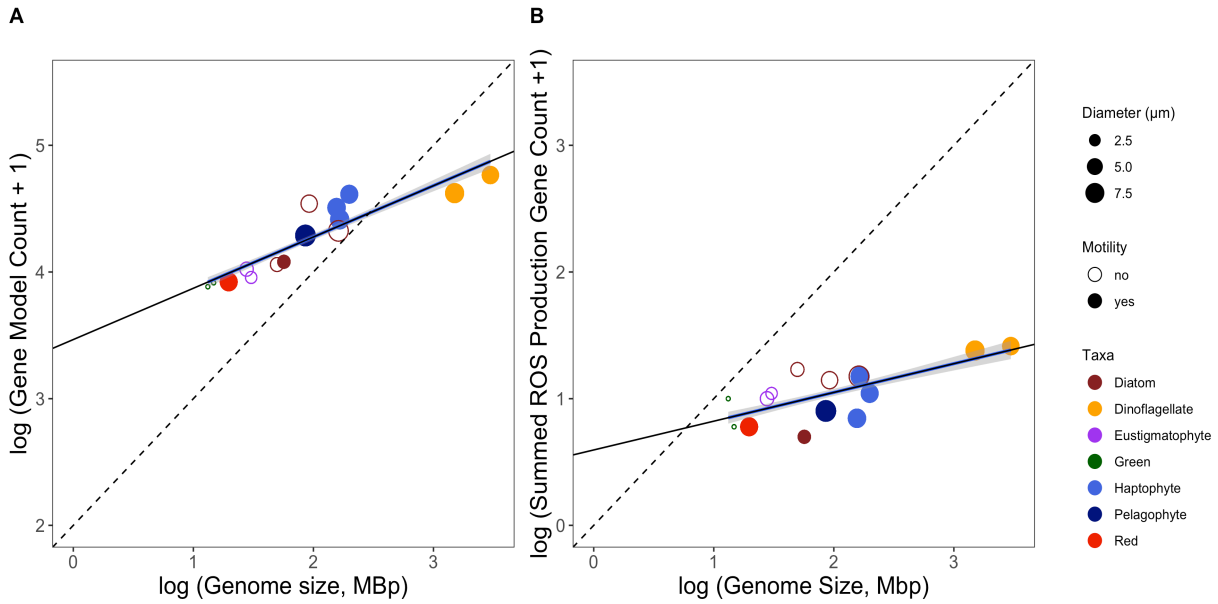

Figure 10: ***Sum of Gene Models and ROS production gene count encoded within each taxon plotted vs. Genome size. A:*** *log10 (Gene Model Count) vs. log10 (Median Cell Diameter (µm)) for those taxa with gene model count data available. Gene model counts for transcriptomic data were assumed equal to the total number of transcribed products detected.,* ***B****: log10 (Sum of ROS detoxification genes) vs. log10 (Median Cell Diameter (µm)) for each taxon. Regression fitted to all data (solid line) with 95% confidence intervals (grey area). Symbol colour corresponds to taxon lineages. Filled symbols indicate species that are motile, which is indicated by the presence or absence of a flagella. Circular symbols represent genomic data and diamond symbols represent transcriptomic data. Citations for data sources in Supplemental Data Table 1.*

In Figure 10A, we compared the gene model count with genome size and found a positive slope of 0.40 ± 0.04. In Figure 10B, the slope between summed ROS Gene Production count was also positive indicating that cells with larger genomes have more genetic capacity to produce more ROS; log10 Summed ROS Gene Production Count +1 vs log10 Genome size was 0.23 ± 0.05.

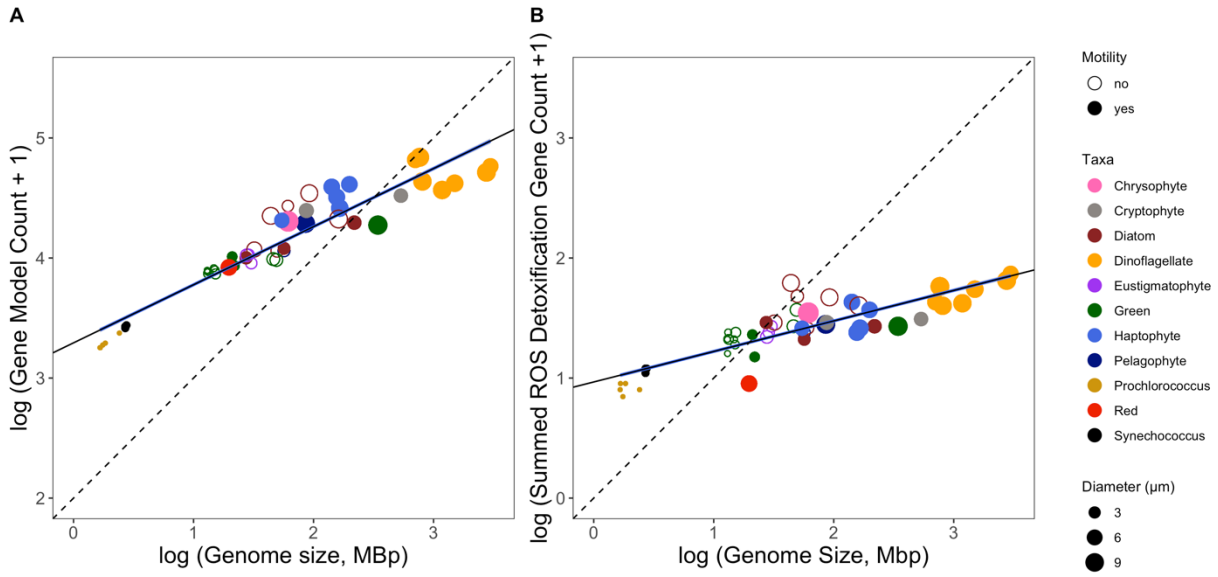

Figure 11: ***Sum of Gene Models and ROS scavenging gene count encoded within each taxon plotted vs. Genome size.*** ***A:*** *log10 (Gene Model Count) vs. log10 (Median Cell Diameter (µm)) for those taxa with gene model count data available. Gene model counts for transcriptomic data were assumed equal to the total number of transcribed products detected.,* ***B:*** *log10 (Sum of ROS detoxification genes) vs. log10 (Median Cell Diameter (µm)) for each taxon. Regression fitted to all data (solid line) with 95% confidence intervals (grey area). Symbol colour corresponds to taxon lineages. Filled symbols indicate species that are motile, which is indicated by the presence or absence of a flagella. Circular symbols represent genomic data and diamond symbols represent transcriptomic data. Citations for data sources in Supplemental Data Table 1.*

Figure 11A compares the gene model count with the genome size and found a slope of 0.48 ± 0.01Mbp. In Figure 11B we compared the total number of ROS scavenging genes with the genome size, and found a slope of 0.25 ± 0.01Mbp.

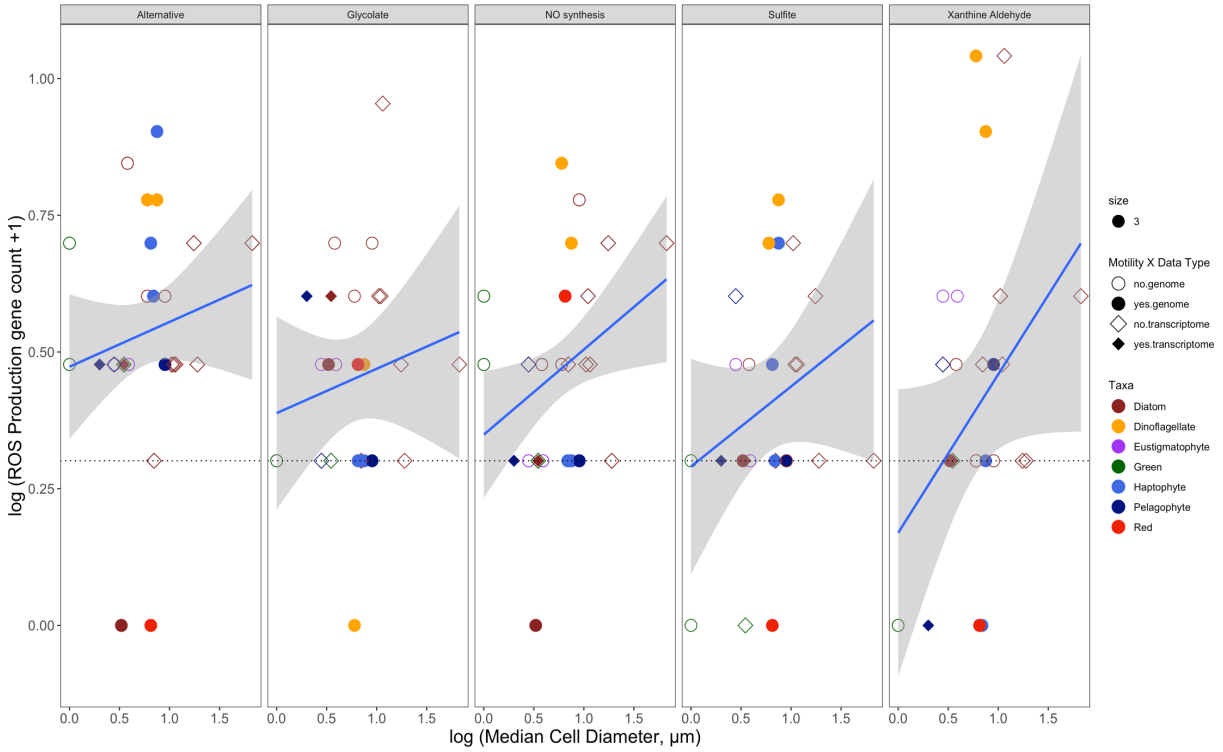

Figure 12: ***log10 (ROS Producing Gene Count +1) for each ROS scavenging enzyme functional group analysed vs. log10 (Median Cell Diameter, µm).*** *The alternative facet includes AOX and PTOX. The glycolate facet solely includes GOX, whereas the NO synthesis facet includes Nitrate reductase and Nitric oxide synthase. The sulfite facet solely includes sulfite oxidase. The Xanthine Aldehyde facet includes both xanthine oxidase and aldehyde oxidase. Solid blue line corresponds to the linear regression between log10 (ROS Producing Gene Count +1) and log10(Median Cell Diameter in µm) within each ROS producing functional group* ± 95% Confidence Intervals (grey area)*. Symbol colour corresponds to taxon lineages. Circular symbols represent genomic data and diamond symbols represent transcriptomic data. Citations for data sources in Supplemental Table 1.*

Figure 12 is a grid comparing ROS production gene count and the cell Diameter across enzyme functional groups. The slope comparing log10 number of ROS production isoforms vs. log10 Cell diameter are as follows; Alternative 0.09 ± 0.14 ($p = 0.29$); Glycolate 0.08 ± 0.19 ($p=0.42$); NO synthesis 0.10 ± 0.13 ($p = 0.02$); Sulfite 0.18 ± 0.20 ($p = 0.02$); Xanthine Aldehyde 0.35 ± 0.29 ($p = 0.06$).

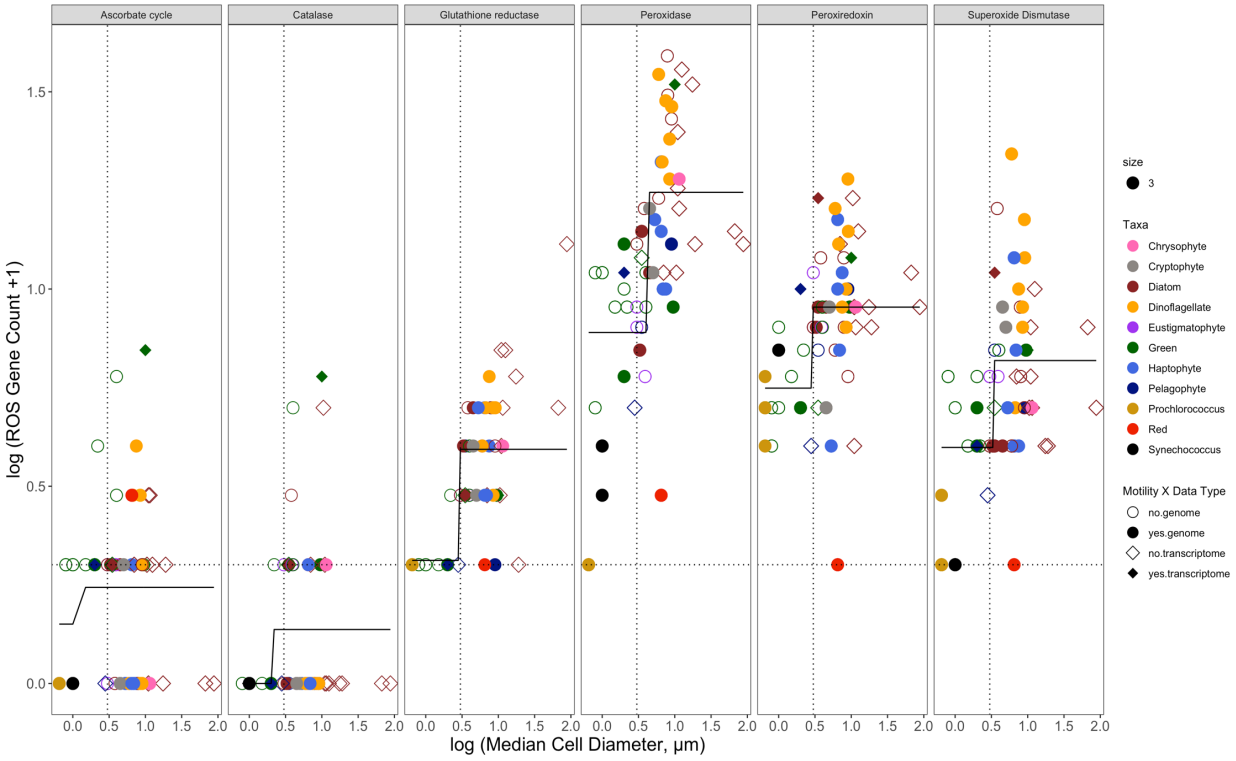

Figure 13: ***log10 (ROS Scavenging Gene Count +1) for each ROS detoxification enzyme functional group analyzed vs. log10 (Median Cell Diameter, µm).*** *Ascorbate cycle facet includes MDHAR and DHAR. Catalase facet includes CAT. Glutathione reductase facet includes GR. Peroxidase facet includes APX, KatG, GPx, and CCP. Peroxiredoxin facet includes PRxQ, typical 2CysPRx, atypical 2CysPRx, and 1CysPRx. Superoxide Dismutase facet includes MnSOD, FeSOD, CuZnSOD, and NiSOD. Solid line indicates stepped threshold. Horizontal dashed line is at 1, whereas points below it are absent. The vertical dashed line is at 3.0µm – the threshold determined in Figure 9. Symbol colour corresponds to taxon lineages. Circular symbols represent genomic data and diamond symbols represent transcriptomic data. Citations for data sources in Supplemental Table 1.*

Figure 13 compares ROS detoxification gene count with the cell diameter in each ROS detoxification enzyme functional group. The step change for the Ascorbate cycle takes place at 1.50µm (p = 0.56); Catalase at 2.20µm (p = 0.38); Glutathione reductase at 3.00µm (p = 3.51E-08); Peroxidase at 4.49µm (p = 0.12); Peroxiredoxin at 3.00µm (p = 3.05E-08); Superoxide dismutase at 3.55µm (p = 3.40E-0.2). Figure 9 which compared all the functional groups summed together found there to be a step change at 3.0µm (p = 6.23E-21).

Within ROS production genes, we found there to be significant interactions ($p < 2e-16$) between the effect of the genome size (Figure 10), and that of the diameter of the cell (Figure 9) on the number of genes responsible for producing ROS. As a result, the p-value of the regression could not be calculated without violating the assumptions behind the regression. The same applies within ROS Scavenging, whereby the p-value of the regression within Figure 9 could not be computed due to significant interactions ($p = 0.02$) between the Diameter effect and total number of genes effect on the number of ROS scavenging genes.

Discussion

Genome vs. transcriptomic data

As larger cells generally have larger genomes (Figure 6), and larger genomes are less frequently sequenced because of the cost and complexity in doing so, genomes of smaller organisms were more frequently available than those of larger organisms. The largest cell for which we found a genome sequenced has a cell diameter of 9.5µm, whereas the largest cell for which we found a transcriptome sequenced has a cell diameter of 88µm, an order of magnitude larger, but still only ~1/5 the size of the largest known phytoplankton cells. Genomes and transcriptomes may provide different information, in that information contained from a transcriptome would vary among different growth conditions as different genes would be expressed. As a result, a negative result from a transcriptome is not conclusive as it could either mean that the gene is not present in the organism genome, or that it was not transcribed under the conditions sampled. In order to identify whether this poses a problem, we analysed paired genomes and transcriptomes from the same organisms. There is no significant difference between the information obtained from a genome, and that from a transcriptome (Figure 7). Theoretically, the transcriptome should not contain any information that is not in the genome, although errors in annotation of the sequences or errors in the algorithm that predicts a protein can arise [181], as found in the genome of *Tisochrysis lutea* where there were occasional doubles of the same gene.

ROS Production and Scavenging genes increase with increasing genome size and cell diameter

As the cell diameter increases, so does the total number of genes carried by the organism (Figures 8A and 9A). Similarly, as the size of the genome increases, so do the total number of genes within the organism. Figure 10A and 11A). This can be explained by the fact that larger cells tend to be more complex, and more complex organisms tend to have more genes [129].

Figure 8B shows that larger cells have more genes that code for the production of ROS; increasing by 1.58 ± 1.14 genes per µm increase in cell diameter. This slope is however smaller than that of Fig. 8A which compares the total number of genes in the genome to cell diameter, which increases by 2.19 ± 1.20 genes per µm increase in cell diameter. This implies a progressively smaller allocation of the genome to ROS producing genes with increasing cell size,

as predicted by our Black Queen hypothesis that large cells will lose less ROS through diffusion than smaller cells. This judgement is however not conclusive as p-values were not be computed on these regressions due to the interaction of cell diameter and genome size. Figure 12 provides a closer insight into the allocations of ROS Producing gene families in the organism genomes. In this figure, for all facets, each consisting of a family of ROS producing genes, all the families except for xanthine aldehyde family had positive correlations which were, however, not significantly different from 0 as indicated by the 95% CI larger than the slopes. This implies that the positive correlation seen in Figure 8B may be as a result of a cumulative add-on effect from each family. Considering that the family-specific slopes are not significantly different from 0, and that there is an interaction between the effect of the diameter and the size of the genome on the total count of ROS producing genes, whereby the number of ROS producing genes increases with increasing genome size. We are unable to determine the actual effect of the diameter of the cell on the ROS producing gene count without further statistics. An ANCOVA that considers the effect of this interaction would uncover the relative influences of cell size and genome upon the gene counts.

Some of the variability in Figure 8 may be attributable to the fact that some of the taxa are bloom-forming. Previous studies have suggested that bloom-forming phytoplankton tend to have higher amounts of ROS production *in vivo* [131], taking this into consideration, bloom forming may be a more meaningful factor than motility.

For ROS scavenging genes, as cells get larger, they also allocate more genes to scavenging ROS (Figure 9). The breakpoint analysis in this figure also revealed that a step change takes place at 3µm which can be explained by the fact that H_2O_2 diffuses ~2µm in its 1ms half-life [130]. In this case, H_2O_2 would readily diffuse out of any cell with a radius less than its diffusion distance (<4µm diameter). Consistent with the Black Queen Hypothesis cells that are a lot smaller than the diffusion distance of H_2O_2 would have no cost to losing the gene that scavenges it, and as a result would be expected to have fewer genes encoding scavenging of H_2O_2. It is however worth considering that a significant interaction ($p = 0.02$) was found between the effect of the diameter of the cell and the total number of genes within the genome. As a result, it would violate assumptions to make a conclusive argument without an ANCOVA that incorporates this interaction.

In Figure 13, gene counts encoding various ROS detoxification enzyme families are compared to the diameters of the cells. As mentioned earlier, Figure 9 estimates that a step change takes place at 3μm which is shown by the vertical line in each panel. Glutathione reductase and peroxiredoxin comply with this step change, with step changes at 3.00μm (p = 3.51E-08) and 3.00μm (p = 3.05E-08) respectively. This is expected as both scavenge H_2O_2. Superoxide also had a significant step change at 3.50μm (p = 3.40E-0.2), which is harder to explain due to the fact that superoxide does not readily diffuse across a membrane [45]. The ascorbate cycle, catalase and peroxidases did not have significant step changes, which can be attributed to the fact that alternate more efficient pathways for ROS detoxification that are in effect; Peroxiredoxins are capable of clearing hydrogen peroxide at both high and low concentrations [132].

Another important consideration that should have been considered is that we used the total number of transcripts as a replacement for the total number of genes when available. Running another paired graph, similar to that of Figure 6, would indicate whether or not there was a difference in the gene model count would validate this assumption.

Conclusions and Future Directions

Previous research has indicated the importance of ROS homeostasis. Some research has analysed loss of function mutations in smaller picocyanobacteria, but not in eukaryotes [1]. This research attempts to answer whether loss of function mutations of ROS detoxification genes take place preferentially in smaller cells, and whether losses of ROS production genes take place preferentially in larger cells. Due to interactions with genome size and total number of genes, additional statistics are needed to answer this question. However, a breakpoint of 3µm was established in the sense that cells smaller than 3µm have fewer ROS detoxification genes, whereas no statistically significant size breaks emerged in plots of ROS detoxification genes vs. genome size. Due to the interaction, a more advanced statistical test such as an ANCOVA is needed, to determine whether ROS production/scavenging genes still increase with increasing cell size when the interacting effect of the genome size is removed.

Future research should look at nitric oxide production in greater detail as it is considered as one of the more important signalling molecules [48]. Analysing the presence/absence of NOFNiR as opposed to NR may yield a more accurate result as NOFNiR directly forms nitric oxide, whereas NR is an enzyme feeding Nitrite into multiple sinks aside from NOFNiR. Additional genes that could be looked at include those linked to tocopherol and carotenoid synthesis, which scavenge ROS non-enzymatically [49,50].

More research is also required on the relative importance of the various enzymes which may lead to a better understanding of a cost/benefit analysis. As ROS signalling in phytoplankton is also underexplored, more research would need to be carried out in the field, which cannot be properly understood until the misunderstanding that ROS is solely a toxic by-product is debunked.

Supplemental Data

Supplemental Table 1: ***Accession information, cell diameter, genome size and gene model count.***

Taxa	Phylogeny	Median Cell Diameter (µm)	Genome Size (Mbp)	Gene Model Count	Database	File Accession Code
Guillardia theta CCMP2712	Cryptophyte	5[133]	87.16	24840	JGI	16067
Fragilariopsis cylindrus CCMP 1102	Diatom	3[134]	61.1	27137	PicoPlaza	proteome.fcy.tfa.gz
Pseudo-nitzschia multistriata B856	Diatom	3.3[135]	56.76	12039	NCBI	ASM90066040v1
Phaeodactylum tricornutum CCAP 1055/1	Diatom	3.5[136]	27.4	10025	NCBI	ASM15095v2
Pseudo-nitzschia multiseries CLN-47	Diatom	4.5[137]	218.73	19703	JGI	1076539
Fistulifera solaris JPCC DA0580	Diatom	3.8[138]	49.74	11448	NCBI	Fsol_1.0
Thalassiosira pseudonana CCMP1335	Diatom	6[139]	32.1	11776	PicoPlaza	proteome.tps.tfa.gz
Thalassiosira oceanica CCMP1005	Diatom	8[139]	92.19	34642	NCBI	PRJNA36595
Skeletonema marinoi -	Diatom	7.9[140]	44	22440	Sequence Server	All models protein
Coscinodiscus wailesii CCMP2513	Diatom	88[141]	N/A	36405	MMETSP	CAM_SMPL_002625
Nitzschia palea -	Diatom	3.5[142]	N/A	15885	ENA	GHBX01000000

Taxa	Phylogeny	Median Cell Diameter (μm)	Genome Size (Mbp)	Gene Model Count	Database	File Accession Code
Leptocylindrus danicus -	Diatom	10.5[143]	N/A	15701	ENA	GAUB01000000
Thalassiosira antarctica CCMP982	Diatom	11[144]	N/A	31618	iMicrobe	Thalassiosira-antarctica-CCMP982.pep.fa.gz
Chaetoceros debilis MM31A_1	Diatom	13[145]	N/A	19453	iMicrobe	Chaetoceros-debilis-MM31A_1.pep.fa.gz
Thalassiosira rotula CCMP3096	Diatom	17.5[146]	N/A	26935	iMicrobe	Thalassiosira-rotula-CCMP3096.pep.fa.gz
Chaetoceros neogracilis CCMP1317	Diatom	3.5[147]	N/A	27860	iMicrobe	Chaetoceros-neogracile-CCMP1317.pep.fa.gz
(Thalassiosira) Conticribra weissflogii CCMP1010	Diatom	11[148]	N/A	21329	iMicrobe	Thalassiosira-weissflogii-CCMP1010.pep.fa.gz
Thalassiosira minuscula CCMP1093	Diatom	12.5[149]	N/A	44803	iMicrobe	Thalassiosira-minuscula-CCMP1093.pep.fa.gz
Ditylum brightwellii GSO103	Diatom	67[150]	N/A	24623	iMicrobe	Ditylu-brightwellii-GSO103.pep.fa.gz
Chaetoceros curvisetus -	Diatom	11.25[151]	N/A	23542	iMicrobe	Chaetoceros-curvisetus .pep.fa.gz
Symbiodinium microadriaticum CCMP2467	Diatom	8.5[152]	808.23	43403	JGI	Symbiodinium microadriaticum CCMP2467
Cyclotella cryptica -	Diatom	9[153]	161.7	21121	UCLA	Nuclear genome

Taxa	Phylogeny	Median Cell Diameter (μm)	Genome Size (Mbp)	Gene Model Count	Database	File Accession Code
(Symbiodinium) Fugacium kawagutii -	Dinoflagellates	8.5[154]	1180	36850	MALAB	Sequences: proteins
(Symbiodinium) Breviolum minutum -	Dinoflagellates	7.5[155]	1500	41925	MGU	symbB.v1.2.augustus.prot.fa.gz
Symbiodinium tridacnidorum -	Dinoflagellates	9.1[156]	766.6	69018	MGU	symA3_37.fasta.gz
(Symbiodinium) Cladocopium goreaui -	Dinoflagellates	6.7[157]	705	65832	MGU	symC_aug_40.aa.gz
Polarella glacialis CCMP1383	Dinoflagellates	6[158]	2980	58232	AARNET	Polarella_glacialis_CCMP1383_PredGene_v1.pep.fa
Polarella glacialis CCMP2088	Dinoflagellates	9[159]	2760	51713	AARNET	Polarella_glacialis_CCMP2088_PredGene_v1.pep.fa
Nannochloropsis oceanica CCMP1779v2	Eustigmatophyceae	3[160]	28.74	10641	JGI	1143084
Nannochloropsis gaditana CCMP526	Eustigmatophyceae	3[161]	30.3	9052	NCBI	ASM24072v1
Microchloropsis salina CCMP1776	Eustigmatophyceae	2.5[162]	27.76	10522	Greenhouse	protein sequence v1
Ostreococcus tauri RCC 1115	Green	1[163]	14.76	8218	NCBI	Ostta1115_2
Ostreococcus tauri OTH95	Green	0.8[164]	13	7892	PicoPlaza	proteome.ota.tfa.gz√ä

Taxa	Phylogeny	Median Cell Diameter (μm)	Genome Size (Mbp)	Gene Model Count	Database	File Accession Code
Ostreococcus tauri RCC4221	Green	1[165]	13.03	7669	NCBI	GCF_000214015.3
Ostreococcus lucimarinus strain CCE9901	Green	1[15]	13.2	7651	JGI	1077109
Ostreococcus - RCC 809v2	Green	2[166]	13.3	7429	JGI	16233
Bathycoccus prasinos RCC 1105	Green	1.5[167]	15.07	7900	PicoPlaza	proteome.bprrcc1105.tfa.gz
Micromonas pusilla CCMP1545	Green	2.5[168]	21.95	8616	PicoPlaza	proteome.mpu.tfa.gz
Micromonas commoda sp. RCC299	Green	2[169]	21	10262	PicoPlaza	proteome.mrcc299.tfa.gz
Picochlorum soloecismus strain DOE101	Green	2.2[170]	15.25	7367	Greenhouse	protein sequence v1
Chlorella variabilis sp. NC64A	Green	4	46.2	9791	JGI	16663
Coccomyxa - sp. C-169	Green	4[171]	49	9629	JGI	1076510
Auxenochlorella protothecoides -	Green	5[172]	22.92	7013	Greenhouse	protein sequence v1
Chlorella sorokiniana UTEX1230	Green	6[173]	58.5	N/A	Greenhouse	protein sequence v1
Pyramimonas parkeae CCAC0082	Green	10[174]	N/A	78786	OneKP	TNAW-SOAPdenovo-Trans-assembly.fa.bz2

Taxa	Phylogeny	Median Cell Diameter (μm)	Genome Size (Mbp)	Gene Model Count	Database	File Accession Code
Chlamydomonas reinhardtii -	Green	10[175]	112.3	16709	JGI	1083931
Dunaliella salina CCAP 19/18	Green	9.5[176]	343.7	18801	JGI	1014865
Picocystis salinarium CCMP1897	Green	3.5[177]	N/A	6947	iMicrobe	Picocystis-salinarum-CCMP1897.pep.fa.gz
Chrysochromulina sp. CCMP291	Haptophytes	5.5[178]	59.07	14777	NCBI	Ctobinv2
Emiliania huxleyi CCMP1516	Haptophytes	6.5[179]	141.7	39126	JGI	16965
Chrysochromulina parva -	Haptophytes	5[106]	65.8	N/A	Greenhouse	protein sequence v1
Pavlovales - CCMP2436	Haptophytes	7.5[180]	165.41	26034	JGI	1079750
Tisochrysis lutea -	Haptophytes	5.3[181]	54.4	20582	SEANOE	Protein_sequencesV1
Ochromonadaceae - CCMP2298	Ochromonadaceae	11.5[182]	61.4	20195	JGI	1014529
Aureococcus anophagefferens CCMP1984	Pelagophyceae	3.5[183]	56.7	11501	JGI	16554
Pelagophyceae - CCMP2097	Pelagophyceae	9[184]	85.82	19402	JGI	1020062
Pelagococcus subviridis CCMP1429	Pelagophyceae	3[185]	N/A	21365	iMicrobe	Pelagococcus-subviridis-CCMP1429.pep.fa.gz
Pelagomonas calceolata CCMP1756	Pelagophyceae	2[186]	N/A	1918	iMicrobe	Pelagomonas-calceolata-CCMP1756.pep.fa.gz

Taxa	Phylogeny	Median Cell Diameter (μm)	Genome Size (Mbp)	Gene Model Count	Database	File Accession Code
Cyanidioschyzon merolae -	Red	2[181]	16	5531	Greenhouse	protein sequence v1
Porphyridium purpureum -	Red	6.5[187]	19.7	8355	RUTGERS	P. purpureum√ägenomic assembly (nucleotide)
Phaeocystis antarctica CCMP1374	Haptophytes	6.5[189]	198.94	41088	JGI	Phaeocystis antarctica CCMP1374 v2.2
Phaeocystis globosa Pg-G	Haptophytes	6.9[188]	155.85	32196	JGI	Phaeocystis globosa Pg-G v2.3: Project: 1070438, Phaglo1_GeneModels_PhytozomeGeneModels_proteins_20190222.aa.fasta.gz

Supplemental Table 2: ***ROS Production Gene Count per Taxon***

Genus	species	strain	Taxa	ome	MitoAOx	NOS	NR	GlyOx	XaAlOx	PTOX	SulOx
Fistulifera	solaris	JPCC DA0580	Diatom	genome	2	0	2	4	2	4	2
Leptocylindrus	danicus	-	Diatom	transcriptome	1	1	1	3	3	1	4
Nannochloropsis	gaditana	CCMP526	Eustigmatophyte	genome	1	0	1	2	3	1	2
Microchloropsis	salina	CCMP1776	Eustigmatophyte	genome	1	0	1	2	3	1	1
Nitzschia	palea	-	Diatom	transcriptome	1	0	1	3	1	1	1
Pavlovales	-	CCMP2436	Haptophyte	genome	1	0	1	1	1	6	4
Pelagophyceae	-	CCMP2097	Pelagophyte	genome	1	0	1	1	2	1	1
Thalassiosira	oceanica	CCMP1005	Diatom	genome	2	1	1	3	1	1	4
Thalassiosira	antarctica	CCMP982	Diatom	transcriptome	1	2	1	3	2	1	2
Thalassiosira	rotula	CCMP3096	Diatom	transcriptome	3	2	2	2	1	1	3
Ostreococcus	lucimarinus	CCE9901	Green	transcriptome	2	1	2	1	0	0	1
(Symbiodinium) Breviolum	minutum	-	Dinoflagellate	genome	3	0	4	2	7	2	5
Chaetoceros	debilis	MM31A_1	Diatom	transcriptome	1	0	1	1	1	1	1

Genus	species	strain	Taxa	ome	MitoAOx	NOS	NR	GlyOx	XaAlOx	PTOX	SulOx
Chaetoceros	neogracilis	CCMP1317	Diatom	transcriptome	0	1	1	1	2	1	1
Chaetoceros	curvisetus	-	Diatom	transcriptome	1	0	2	8	10	1	2
Pelagococcus	subviridis	CCMP1429	Pelagophyte	transcriptome	1	1	1	1	2	1	3
Ditylum	brightwellii	GSO103	Diatom	transcriptome	1	1	3	2	3	3	1
Picocystis	salinarium	CCMP1897	Green	transcriptome	2	0	1	1	1	0	0
Phaeocystis	globosa	Pg-G	Haptophyte	genome	2	0	1	1	0	1	1
Phaeocystis	antarctica	CCMP1374	Haptophyte	genome	3	1	2	1	0	1	2
Pseudo-nitzschia	multistriata	B856	Diatom	genome	0	0	0	2	1	0	1
Pelagomonas	calceolata	CCMP1756	Pelagophyte	transcriptome	1	0	1	3	0	1	1
Polarella	glacialis	CCMP1383	Dinoflagellate	genome	2	0	6	0	10	3	4
Micromonas	pusilla	CCMP1545	Green	transcriptome	1	0	2	2	0	1	0
Emiliania	huxleyi	CCMP1516	Haptophyte	transcriptome	4	0	0	0	9	1	3
Porphyridium	purpureum	CCMP1328	Red	genome	0	0	3	2	0	0	0
Ostreococcus	tauri	RCC 1115	Green	genome	1	1	1	1	0	1	0
Cyclotella	cryptica	CCMP332	Diatom	genome	2	0	5	4	1	1	1

Genus	species	strain	Taxa	ome	MitoAOx	NOS	NR	GlyOx	XaAlOx	PTOX	SulOx
Ostreococcus	lucimarinus	CCE9901	Green	genome	3	1	2	1	0	1	1

Supplemental Table 3: ***ROS Scavenging Gene Count per Taxon***

Genus	species	strain	Taxa	ome	FeSOD	MnSOD	CuZnSOD	NiSOD	APX	MDHAR	DHAR	GR	CAT	Katg	GPx	PrxQ	Typ2CysPrx	ATyp2CysPrx	OneCysPrx	CCP
Ostreococcus	tauri	RCC1115	Green	genome	0	1	3	0	3	1	0	1	0	0	6	1	1	2	0	1
Ostreococcus	tauri	OTH95/RCC745	Green	genome	0	1	3	1	3	1	0	1	0	0	6	1	1	1	0	1
Ostreococcus	tauri	RCC4221	Green	genome	0	1	3	1	2	1	0	1	0	0	1	1	2	1	0	1
Ostreococcus	lucimarinus	CCE9901	Green	genome	0	1	2	1	3	1	0	1	0	0	6	1	3	3	0	1
Ostreococcus	sp.	RCC809	Green	genome	0	1	3	1	3	1	0	1	0	0	5	2	1	1	0	1
Bathycoccus	prasinos	RCC1105	Green	genome	0	1	2	0	2	1	0	1	0	0	4	1	1	2	1	2
Micromonas	pusilla	CCMP1545	Green	genome	0	1	2	0	3	1	0	1	0	0	1	2	1	1	0	1
Micromonas	commoda	RCC299	Green	genome	0	1	2	1	5	1	0	1	0	0	5	2	1	1	0	2

Genus	species	strain	Taxa	ome	FeSOD	MnSOD	CuZnSOD	NiSOD	APX	MDHAR	DHAR	GR	CAT	Katg	GPx	PrxQ	Typ2CysPrx	ATyp2CysPrx	OneCysPrx	CCP
Picochlorum	soloecismus	DOE101	Green	genome	1	2	0	0	4	2	1	2	1	0	3	2	2	2	0	1
Aureococcus	anophagefferens	CCMP1984	Pelagophyte	genome	0	2	2	2	0	1	0	3	0	0	4	1	0	2	3	3
Nannochloropsis	oceanica	CCMP1779	Eustigmatophyte	genome	2	1	2	0	3	0	0	2	1	0	4	2	2	3	0	1
Nannochloropsis	gaditana	CCMP526	Eustigmatophyte	genome	2	0	3	0	3	0	1	2	1	0	3	2	4	4	0	1
Fragilariopsis	cylindrus	CCMP1102	Diatom	genome	0	2	1	0	4	0	1	2	0	2	4	2	1	4	0	2
Pseudo-nitzschia	multistriata	B856	Diatom	genome	0	1	1	1	4	0	1	3	0	1	0	1	0	5	1	1
Phaeodactylum	tricornutum	CCAP1055/1	Diatom	genome	0	2	1	0	5	0	1	2	1	1	3	2	1	3	2	4
Pseudo-nitzschia	multiseries	CLN-47	Diatom	genome	0	2	1	0	3	0	1	4	0	1	3	2	0	5	1	3

Genus	species	strain	Taxa	ome	FeSOD	MnSOD	CuZnSOD	NiSOD	APX	MDHAR	DHAR	GR	CAT	Katg	GPx	PrxQ	Typ2CysPrx	ATyp2CysPrx	OneCysPrx	CCP
Fistulifera	solaris	JPCCDA0580	Diatom	genome	0	4	2	9	6	0	0	4	2	0	5	2	0	7	2	4
Microchloropsis	salina	CCMP1776	Eustigmatophyte	genome	2	0	3	0	2	0	1	2	1	0	2	2	1	4	0	1
Pelagophyceae	-	CCMP2097	Pelagophyte	genome	0	2	1	1	5	1	0	1	0	3	4	3	0	3	3	0
Chlorella	variabilis	NC64A	Green	genome	2	4	0	0	2	0	2	2	1	0	5	1	2	3	1	1
Coccomyxa	sp.	C-169	Green	genome	1	5	0	0	6	2	3	3	4	0	3	3	2	1	2	1
Emiliania	huxleyi	CCMP1516	Haptophyte	genome	0	2	0	1	1	0	1	4	0	1	9	3	0	8	3	9
Pavlovales	-	CCMP2436	Haptophyte	genome	1	2	0	0	4	0	0	3	0	0	3	1	1	7	1	2
Thalassiosira	pseudonana	CCMP1335	Diatom	genome	1	2	0	0	7	0	0	3	0	1	2	2	1	2	1	6
Thalassiosira	oceanica	CCMP1005	Diatom	genome	1	2	0	2	17	0	0	4	0	4	7	0	1	5	1	2
Skeletonema	marinoi	-	Diatom	genome	4	3	0	1	25	0	0	4	0	5	5	8	0	2	1	3

Genus	species	strain	Taxa	ome	FeSOD	MnSOD	CuZnSOD	NiSOD	APX	MDHAR	DHAR	GR	CAT	Katg	GPx	PrxQ	Typ2CysPrx	ATyp2CysPrx	OneCysPrx	CCP
Pyramimonas	parkeae	CCAC0082	Green	transcriptome	1	1	4	0	18	6	0	2	5	0	10	1	3	3	4	4
Dunaliella	salina	CCAP19/18	Green	genome	2	4	0	0	5	1	0	2	1	0	3	3	3	2	0	0
Coscinodiscus	wailesii	CCMP2513	Diatom	transcriptome	1	2	1	0	5	0	0	12	0	1	4	2	0	5	1	2
Nitzschia	palea	-	Diatom	transcriptome	1	3	1	5	6	0	1	2	0	1	4	5	0	9	2	2
Leptocylindrus	danicus	-	Diatom	transcriptome	0	2	1	1	3	0	1	2	4	3	2	4	0	4	8	2
Thalassiosira	antarctica	CCMP982	Diatom	transcriptome	3	3	1	0	13	0	0	6	1	3	6	4	0	3	1	2
Chaetoceros	debilis	MM31A_1	Diatom	transcriptome	0	2	0	1	3	0	1	1	0	2	6	2	0	5	0	1
Thalassiosira	rotula	CCMP3096	Diatom	transcriptome	0	2	0	1	16	0	0	5	0	4	6	5	0	3	0	6

Genus	species	strain	Taxa	ome	FeSOD	MnSOD	CuZnSOD	NiSOD	APX	MDHAR	DHAR	GR	CAT	Katg	GPx	PrxQ	Typ2CysPrx	ATyp2CysPrx	OneCysPrx	CCP
Chaetoceros	neogracilis	CCMP1317	Diatom	transcriptome	0	3	0	2	4	0	1	2	1	1	3	2	0	7	3	2
(Thalassiosira) Conticribra	weissflogii	CCMP1010	Diatom	transcriptome	1	2	0	2	10	0	2	3	0	2	2	0	0	3	0	3
Thalassiosira	minuscula	CCMP1093	Diatom	transcriptome	7	2	0	0	15	0	1	6	0	8	6	4	0	5	4	6
Ditylum	brightwellii	GSO103	Diatom	transcriptome	1	2	1	3	7	0	0	4	0	0	3	2	0	6	2	3
Chaetoceros	curvisetus	-	Diatom	transcriptome	1	2	0	1	4	0	2	4	0	2	5	1	0	4	2	4
Symbiodinium	microadriaticum	CCMP2467	Dinoflagellate	genome	0	3	0	5	12	2	0	4	0	2	2	1	1	4	1	2
(Symbiodinium) Fugacium	kawagutii	-	Dinoflagellate	genome	0	4	1	2	18	0	0	2	0	3	1	1	2	5	1	1

Genus	species	strain	Taxa	ome	FeSOD	MnSOD	CuZnSOD	NiSOD	APX	MDHAR	DHAR	GR	CAT	Katg	GPx	PrxQ	Typ2CysPrx	ATyp2CysPrx	OneCysPrx	CCP
(Symbiodinium) Breviolum	minutum	-	Dinoflagellate	genome	0	4	0	5	16	2	1	5	0	5	1	1	2	5	0	7
Symbiodinium	tridacnidorum	clade A3 (Y-106)	Dinoflagellate	genome	0	2	0	9	19	1	0	4	0	4	3	3	3	5	2	2
(Symbiodinium) Cladocopium	goreaui	clade C (Y103)	Dinoflagellate	genome	0	2	0	2	11	1	1	4	0	2	4	4	3	4	1	3
Pelagococcus	subviridis	CCMP1429	Pelagophyte	transcriptome	0	1	0	1	2	0	0	1	0	0	1	1	0	2	0	1
Pelagomonas	calceolata	CCMP1756	Pelagophyte	transcriptome	0	2	0	1	3	1	0	1	0	0	4	2	0	5	2	3
Picocystis	salinarium	CCMP1897	Green	transcriptome	2	2	0	0	6	1	0	2	1	0	4	1	2	1	0	1
Ochromonadaceae	sp.	CCMP2298	Chrysophyte	genome	2	0	2	0	5	0	0	3	1	2	9	3	1	2	2	2

Genus	species	strain	Taxa	ome	Fe SOD	MnSOD	CuZnSOD	NiSOD	APX	MDHAR	DHAR	GR	CAT	Katg	GPx	PrxQ	Typ2CysPrx	ATyp2CysPrx	OneCysPrx	CCP
Tisochrysis	lutea	-	Haptophyte	genome	0	1	1	2	4	0	0	4	0	0	4	0	0	3	0	6
Guillardia	theta	CCMP2712	Cryptophyte	genome	1	4	0	2	4	0	1	2	0	1	3	1	1	6	0	2
Cyclotella	cryptica	CCMP332	Diatom	genome	1	2	0	1	13	0	1	3	0	1	7	3	0	2	0	5
Porphyridium	purpureum	CCMP1328	Red	genome	0	1	0	0	1	1	1	1	1	0	1	0	1	0	0	0
Polarella	glacialis	CCMP1383	Dinoflagellate	genome	0	7	8	6	18	0	0	3	0	7	5	2	2	11	0	4
Polarella	glacialis	CCMP2088	Dinoflagellate	genome	0	2	6	6	12	0	0	4	0	7	5	1	2	14	1	4
Cryptophyceae	sp.	CCMP2293	Cryptophyte	genome	3	2	2	1	5	0	0	3	0	0	7	2	0	2	0	3
Prochlorococcus	marinus	AS9601	Prochlorococcus	genome	1	0	0	1	0	0	0	1	0	0	1	3	1	0	0	0
Prochlorococcus	marinus	CCMP1375	Prochlorococcus	genome	0	0	0	1	0	0	0	1	0	0	1	2	1	0	0	0

Genus	species	strain	Taxa	ome	Fe SOD	MnSOD	CuZnSOD	NiSOD	APX	MDHAR	DHAR	GR	CAT	Katg	GPx	PrxQ	Typ2CysPrx	ATyp2CysPrx	OneCysPrx	CCP
Prochlorococcus	marinus	MIT9313	Prochlorococcus	genome	0	0	0	1	0	0	0	1	0	0	1	3	1	0	0	0
Prochlorococcus	marinus	NATL2A	Prochlorococcus	genome	0	0	0	1	0	0	0	1	0	0	1	4	1	0	0	0
Prochlorococcus	marinus	CCMP1986	Prochlorococcus	genome	0	0	0	1	0	0	0	1	0	0	1	3	1	0	0	0
Emiliania	huxleyi	CCMP1516	Haptophyte	transcriptome	0	2	0	2	2	0	0	4	0	2	13	5	0	9	4	8
Nannochloropsis	gaditana	CCMP526	Eustigmatophyte	transcriptome	0	0	2	0	1	0	0	1	0	0	0	1	1	3	1	0
Thalassiosira	pseudonana	CCMP1335	Diatom	transcriptome	2	2	0	0	8	0	1	3	0	1	2	2	1	3	1	5
Ostreococcus	lucimarinus	CCE9901	Green	transcriptome	0	1	2	1	2	1	0	1	0	0	1	1	3	1	0	2
Phaeodactylum	tricornutum	CCAP1055/1	Diatom	transcriptome	0	2	1	0	6	0	1	2	1	1	3	2	0	4	2	3

Genus	species	strain	Taxa	ome	Fe SOD	MnSOD	CuZnSOD	NiSOD	APX	MDHAR	DHAR	GR	CAT	Katg	GPx	PrxQ	Typ2CysPrx	ATyp2CysPrx	OneCysPrx	CCP
Micromonas	pusilla	CCMP1545	Green	transcriptome	0	1	2	1	5	1	0	1	0	0	5	2	1	2	0	1
(Symbiodinium) Breviolum	minutum	-	Dinoflagellate	transcriptome	0	5	1	4	15	1	0	2	0	7	10	2	2	9	1	3
Synechococcus	elongatus	PCC6301	Synechococcus	genome	1	0	0	0	0	0	0	1	0	1	1	4	1	0	1	0
Symbiodinium	tridacnidorum	clade A3 (Y-106)	Dinoflagellate	transcriptome	0	2	0	3	19	1	0	5	0	3	3	1	3	5	2	3
Fragilariopsis	cylindrus	CCMP1102	Diatom	transcriptome	0	3	2	1	6	0	0	3	0	4	9	4	0	9	0	4
Thalassiosira	oceanica	CCMP1005	Diatom	transcriptome	1	2	0	1	14	0	0	4	0	5	5	0	1	7	1	3
Synechococcus	elongatus	PCC7942	Synechococcus	genome	1	0	0	0	0	0	0	1	0	2	1	4	1	0	1	0

Genus	species	strain	Taxa	ome	FeSOD	MnSOD	CuZnSOD	NiSOD	APX	MDHAR	DHAR	GR	CAT	Katg	GPx	PrxQ	Typ2CysPrx	ATyp2CysPrx	OneCysPrx	CCP
Synechococcus	elongatus	PCC11802	Synechococcus	genome	1	0	0	0	0	0	0	1	0	2	1	4	0	0	2	0
Guillardia	theta	CCMP2712	Cryptophyte	transcriptome	1	4	0	2	4	0	1	2	0	0	3	1	1	6	0	2
Phaeocystis	globosa	Pg-G	Haptophyte	genome	0	2	1	3	1	0	0	2	0	1	5	2	0	3	1	2
Phaeocystis	antarctica	CCMP1374	Haptophyte	genome	0	2	8	1	1	0	0	2	1	4	5	3	0	5	1	3
Pavlovales	-	CCMP2436	Haptophyte	transcriptome	0	3	0	0	4	0	0	3	0	0	3	1	3	7	1	2

Bibliography

1. Morris JJ, Lenski RE, Zinser ER. The Black Queen Hypothesis: Evolution of Dependencies through Adaptive Gene Loss. mBio. 2012;3: e00036–12–e00036–12. doi:10.1128/mBio.00036-12

2. Reynolds CS. The Ecology of Phytoplankton. Cambridge University Press; 2006.

3. Vanni MJ, Luecke C, Kitchell JF, Allen Y, Temte J, Magnuson JJ. Effects on lower trophic levels of massive fish mortality. Nature. 1990;344: 333–335. doi:10.1038/344333a0

4. Simon N, Cras A-L, Foulon E, Lemée R. Diversity and evolution of marine phytoplankton. Comptes Rendus Biologies. 2009;332: 159–170. doi:10.1016/j.crvi.2008.09.009

5. Falkowski P, Knoll AH. Evolution of Primary Producers in the Sea. Academic Press; 2011.

6. Falkowski PG. The role of phytoplankton photosynthesis in global biogeochemical cycles. Photosynthesis Research. 1994;39: 235–258. doi:10.1007/BF00014586

7. Paerl HW. 5.2 Morphological and Ecophysiological Diversity. 2012.

8. Scanlan DJ. Marine Picocyanobacteria. In: Whitton BA, editor. Ecology of Cyanobacteria II: Their Diversity in Space and Time. Dordrecht: Springer Netherlands; 2012. pp. 503–533. doi:10.1007/978-94-007-3855-3_20

9. Falkowski PG, Katz ME, Knoll AH, Quigg A, al et. The Evolution of Modern Eukaryotic Phytoplankton. Science; Washington. 2004;305: 354–60.

10. Leliaert F, Smith DR, Moreau H, Herron MD, Verbruggen H, Delwiche CF, et al. Phylogeny and Molecular Evolution of the Green Algae. Critical Reviews in Plant Sciences. 2012;31: 1–46. doi:10.1080/07352689.2011.615705

11. Ulvskov P, Paiva DS, Domozych D, Harholt J. Classification, Naming and Evolutionary History of Glycosyltransferases from Sequenced Green and Red Algal Genomes. PLoS ONE. 2013;8. doi:10.1371/journal.pone.0076511

12. De Clerck O, Bogaert KA, Leliaert F. Chapter Two - Diversity and Evolution of Algae: Primary Endosymbiosis. In: Piganeau G, editor. Advances in Botanical Research. Academic Press; 2012. pp. 55–86. doi:10.1016/B978-0-12-391499-6.00002-5

13. Reyes-Prieto A, Russell S, Figueroa-Martinez F, Jackson C. Chapter Four - Comparative Plastid Genomics of Glaucophytes. In: Chaw S-M, Jansen RK, editors. Advances in Botanical Research. Academic Press; 2018. pp. 95–127. doi:10.1016/bs.abr.2017.11.012

14. Lemieux C, Otis C, Turmel M. A clade uniting the green algae Mesostigma viride and Chlorokybus atmophyticus represents the deepest branch of the Streptophyta in chloroplast genome-based phylogenies. BMC Biology. 2007;5: 2. doi:10.1186/1741-7007-5-2

15. Palenik B, Grimwood J, Aerts A, Rouzé P, Salamov A, Putnam N, et al. The tiny eukaryote *Ostreococcus* provides genomic insights into the paradox of plankton speciation. Proceedings of the National Academy of Sciences. 2007;104: 7705–7710. doi:10.1073/pnas.0611046104

16. Santos AL dos, Pollina T, Gourvil P, Corre E, Marie D, Garrido JL, et al. Chloropicophyceae, a new class of picophytoplanktonic prasinophytes. Scientific Reports. 2017;7: 1–20. doi:10.1038/s41598-017-12412-5

17. Levine I, Fleurence J, editors. Microalgae in health and disease prevention. San Diego: Academic Press, an imprint of Elsevier; 2018.

18. Keeling PJ. The endosymbiotic origin, diversification and fate of plastids. Philosophical Transactions of the Royal Society B: Biological Sciences. 2010;365: 729–748. doi:10.1098/rstb.2009.0103

19. Yoon HS, Muller KM, Sheath RG, Ott FD, Bhattacharya D. DEFINING THE MAJOR LINEAGES OF RED ALGAE (RHODOPHYTA)1. Journal of Phycology. 2006;42: 482–492. doi:10.1111/j.1529-8817.2006.00210.x

20. Iovinella M, Eren A, Pinto G, Pollio A, Davis SJ, Cennamo P, et al. Cryptic dispersal of Cyanidiophytina (Rhodophyta) in non-acidic environments from Turkey. Extremophiles: Life Under Extreme Conditions. 2018;22: 713–723. doi:10.1007/s00792-018-1031-x

21. Nicholls KH. Chapter 13 - Haptophyte Algae. In: Wehr JD, Sheath RG, Kociolek JP, editors. Freshwater Algae of North America (Second Edition). Boston: Academic Press; 2015. pp. 587–605. doi:10.1016/B978-0-12-385876-4.00013-X

22. Gross M. The mysteries of the diatoms. Current Biology. 2012;22: R581–R585. doi:10.1016/j.cub.2012.07.041

23. Čalija B, editor. Microsized and nanosized carriers for nonsteroidal anti-inflammatory drugs: Formulation challenges and potential benefits. London: Academic Press, an imprint of Elsevier; 2017.

24. Round FE, Crawford RM, Mann DG. Diatoms: Biology and Morphology of the Genera. Cambridge University Press; 1990.

25. Medlin LK, Kaczmarska I. Evolution of the diatoms: V. Morphological and cytological support for the major clades and a taxonomic revision. Phycologia. 2004;43: 245–270. doi:10.2216/i0031-8884-43-3-245.1

26. Yu M, Ashworth MP, Hajrah NH, Khiyami MA, Sabir MJ, Alhebshi AM, et al. Chapter Five - Evolution of the Plastid Genomes in Diatoms. In: Chaw S-M, Jansen RK, editors. Advances in Botanical Research. Academic Press; 2018. pp. 129–155. doi:10.1016/bs.abr.2017.11.009

27. Wisecaver JH, Hackett JD. Dinoflagellate genome evolution. Annual Review of Microbiology. 2011;65: 369–387. doi:10.1146/annurev-micro-090110-102841

28. Janouškovec J, Gavelis GS, Burki F, Dinh D, Bachvaroff TR, Gornik SG, et al. Major transitions in dinoflagellate evolution unveiled by phylotranscriptomics. Proceedings of the National Academy of Sciences. 2017;114: E171–E180. doi:10.1073/pnas.1614842114

29. Schmid A-MM, Volcani BE. WALL MORPHOGENESIS IN COSCINODISCUS WAILESII GRAN AND ANGST. I. VALVE MORPHOLOGY AND DEVELOPMENT OF ITS

ARCHITECTURE1. Journal of Phycology. 1983;19: 387–402. doi:10.1111/j.0022-3646.1983.00387.x

30. Palenik B. Molecular Mechanisms by Which Marine Phytoplankton Respond to Their Dynamic Chemical Environment. Annual Review of Marine Science. 2015;7: 325–340. doi:10.1146/annurev-marine-010814-015639

31. Morán XAG, López-Urrutia Á, Calvo-Díaz A, Li WKW. Increasing importance of small phytoplankton in a warmer ocean. Global Change Biology. 2010;16: 1137–1144. doi:10.1111/j.1365-2486.2009.01960.x

32. Rasconi S, Gall A, Winter K, Kainz MJ. Increasing Water Temperature Triggers Dominance of Small Freshwater Plankton. PLoS ONE. 2015;10. doi:10.1371/journal.pone.0140449

33. Rasconi S, Winter K, Kainz MJ. Temperature increase and fluctuation induce phytoplankton biodiversity loss from a multi-seasonal mesocosm experiment. Ecology and Evolution. 2017;7: 2936–2946. doi:10.1002/ece3.2889

34. Bayr H. Reactive oxygen species: Critical Care Medicine. 2005;33: S498–S501. doi:10.1097/01.CCM.0000186787.64500.12

35. Sharma P, Jha AB, Dubey RS, Pessarakli M. Reactive Oxygen Species, Oxidative Damage, and Antioxidative Defense Mechanism in Plants under Stressful Conditions. Journal of Botany. 2012;2012: e217037. doi:10.1155/2012/217037

36. Das K, Roychoudhury A. Reactive oxygen species (ROS) and response of antioxidants as ROS-scavengers during environmental stress in plants. Frontiers in Environmental Science. 2014;2. doi:10.3389/fenvs.2014.00053

37. Mittler R. ROS Are Good. Trends in Plant Science. 2017;22: 11–19. doi:10.1016/j.tplants.2016.08.002

38. Signorelli S, Tarkowski ŁP, Van den Ende W, Bassham DC. Linking Autophagy to Abiotic and Biotic Stress Responses. Trends in Plant Science. 2019;24: 413–430. doi:10.1016/j.tplants.2019.02.001

39. Apel K, Hirt H. REACTIVE OXYGEN SPECIES: Metabolism, Oxidative Stress, and Signal Transduction. Annual Review of Plant Biology. 2004;55: 373–399. doi:10.1146/annurev.arplant.55.031903.141701

40. Marino D, Dunand C, Puppo A, Pauly N. A burst of plant NADPH oxidases. Trends in Plant Science. 2012;17: 9–15. doi:10.1016/j.tplants.2011.10.001

41. Ray PD, Huang B-W, Tsuji Y. Reactive oxygen species (ROS) homeostasis and redox regulation in cellular signaling. Cellular signalling. 2012;24: 981–990. doi:10.1016/j.cellsig.2012.01.008

42. Halliwell B, Gutteridge JMC. Free radicals in biology and medicine. 3rd ed. Oxford : New York: Clarendon Press ; Oxford University Press; 1999.

43. Li R, Jia Z, Trush MA. Defining ROS in Biology and Medicine. Reactive oxygen species (Apex, NC). 2016;1: 9–21. doi:10.20455/ros.2016.803

44. Collin F. Chemical Basis of Reactive Oxygen Species Reactivity and Involvement in Neurodegenerative Diseases. International Journal of Molecular Sciences. 2019;20. doi:10.3390/ijms20102407

45. Hansel CM, Buchwald C, Diaz JM, Ossolinski JE, Dyhrman ST, Mooy BASV, et al. Dynamics of extracellular superoxide production by Trichodesmium colonies from the Sargasso Sea. Limnology and Oceanography. 2016;61: 1188–1200. doi:10.1002/lno.10266

46. Chamizo-Ampudia A, Sanz-Luque E, Llamas A, Galvan A, Fernandez E. Nitrate Reductase Regulates Plant Nitric Oxide Homeostasis. Trends in Plant Science. 2017;22: 163–174. doi:10.1016/j.tplants.2016.12.001

47. Gross L. Diatoms Rely on Sophisticated Signaling Systems for Population Control. PLOS Biology. 2006;4: e89. doi:10.1371/journal.pbio.0040089

48. Fu Y-F, Zhang Z-W, Yuan S. Putative Connections Between Nitrate Reductase S-Nitrosylation and NO Synthesis Under Pathogen Attacks and Abiotic Stresses. Frontiers in Plant Science. 2018;9. doi:10.3389/fpls.2018.00474

49. Mallick N, Mohn FH. Reactive oxygen species: Response of algal cells. Journal of Plant Physiology. 2000;157: 183–193. doi:10.1016/S0176-1617(00)80189-3

50. Yildiz G, Vatan Ö, Çelikler S, Dere Ş. Determination of the Phenolic Compounds and Antioxidative Capacity in Red Algae Gracilaria bursa-pastoris. International Journal of Food Properties. 2011;14: 496–502. doi:10.1080/10942910903256949

51. Bowler C, Camp WV, Montagu MV, Inzé D, Asada PK. Superoxide Dismutase in Plants. Critical Reviews in Plant Sciences. 1994;13: 199–218. doi:10.1080/07352689409701914

52. Wolfe-Simon F, Grzebyk D, Schofield O, Falkowski PG. The Role and Evolution of Superoxide Dismutases in Algae1. Journal of Phycology. 2005;41: 453–465. doi:10.1111/j.1529-8817.2005.00086.x

53. Alscher RG, Erturk N, Heath LS. Role of superoxide dismutases (SODs) in controlling oxidative stress in plants. Journal of Experimental Botany. 2002;53: 1331–1341. doi:10.1093/jxb/53.372.1331

54. Case AJ. On the Origin of Superoxide Dismutase: An Evolutionary Perspective of Superoxide-Mediated Redox Signaling. Antioxidants. 2017;6. doi:10.3390/antiox6040082

55. Yan H, Harding JJ. Glycation-induced inactivation and loss of antigenicity of catalase and superoxide dismutase. Biochemical Journal. 1997;328: 599–605.

56. Gottfredsen RH, Larsen UG, Enghild JJ, Petersen SV. Hydrogen peroxide induce modifications of human extracellular superoxide dismutase that results in enzyme inhibition. Redox Biology. 2013;1: 24–31. doi:10.1016/j.redox.2012.12.004

57. Pandey P, Singh J, Achary VMM, Reddy MK. Redox homeostasis via gene families of ascorbate-glutathione pathway. Frontiers in Environmental Science. 2015;3. doi:10.3389/fenvs.2015.00025

58. Gallie DR. The role of l-ascorbic acid recycling in responding to environmental stress and in promoting plant growth. Journal of Experimental Botany. 2013;64: 433–443. doi:10.1093/jxb/ers330

59. Bartoli CG, Buet A, Gergoff Grozeff G, Galatro A, Simontacchi M. Ascorbate-Glutathione Cycle and Abiotic Stress Tolerance in Plants. In: Hossain MA, Munné-Bosch S, Burritt DJ, Diaz-Vivancos P, Fujita M, Lorence A, editors. Ascorbic Acid in Plant Growth, Development and Stress Tolerance. Cham: Springer International Publishing; 2017. pp. 177–200. doi:10.1007/978-3-319-74057-7_7

60. Sofo A, Scopa A, Nuzzaci M, Vitti A. Ascorbate Peroxidase and Catalase Activities and Their Genetic Regulation in Plants Subjected to Drought and Salinity Stresses. International Journal of Molecular Sciences. 2015;16: 13561–13578. doi:10.3390/ijms160613561

61. Ozyigit II, Filiz E, Vatansever R, Kurtoglu KY, Koc I, Öztürk MX, et al. Identification and Comparative Analysis of H2O2-Scavenging Enzymes (Ascorbate Peroxidase and Glutathione Peroxidase) in Selected Plants Employing Bioinformatics Approaches. Frontiers in Plant Science. 2016;7. doi:10.3389/fpls.2016.00301

62. Halliwell B, Gutteridge JMC. Free radicals in biology and medicine. Fifth edition. Oxford, United Kingdom: Oxford University Press; 2015.

63. Bhaskar B, Lad L, Poulos TL. Iron: Heme Proteins, Peroxidases, Catalases & Catalase-Peroxidases Based in part on the article Iron: Heme Proteins, Peroxidases, & Catalases by Ann M. English which appeared in the Encyclopedia of Inorganic Chemistry, First Edition. Encyclopedia of Inorganic Chemistry. American Cancer Society; 2006. doi:10.1002/0470862106.ia106

64. Shimizu N, Kobayashi K, Hayashi K. The reaction of superoxide radical with catalase. Mechanism of the inhibition of catalase by superoxide radical. The Journal of Biological Chemistry. 1984;259: 4414–4418.

65. Djordjević VB. Free Radicals in Cell Biology. International Review of Cytology. Academic Press; 2004. pp. 57–89. doi:10.1016/S0074-7696(04)37002-6

66. Hasanuzzaman M, Nahar K, Anee TI, Fujita M. Glutathione in plants: Biosynthesis and physiological role in environmental stress tolerance. Physiology and Molecular Biology of Plants. 2017;23: 249–268. doi:10.1007/s12298-017-0422-2

67. Chouchane S, Lippai I, Magliozzo RS. Catalase-Peroxidase (*Mycobacterium Tuberculosis* KatG) Catalysis and Isoniazid Activation . Biochemistry. 2000;39: 9975–9983. doi:10.1021/bi0005815

68. Passardi F, Zamocky M, Favet J, Jakopitsch C, Penel C, Obinger C, et al. Phylogenetic distribution of catalase-peroxidases: Are there patches of order in chaos? Gene. 2007;397: 101–113. doi:10.1016/j.gene.2007.04.016

69. Martins D, Kathiresan M, English AM. Cytochrome c peroxidase is a mitochondrial heme-based H2O2 sensor that modulates antioxidant defense. Free Radical Biology & Medicine. 2013;65: 541–551. doi:10.1016/j.freeradbiomed.2013.06.037

70. Erman JE, Vitello LB. Yeast cytochrome c peroxidase: Mechanistic studies via protein engineering. Biochimica et Biophysica Acta (BBA) - Protein Structure and Molecular Enzymology. 2002;1597: 193–220. doi:10.1016/S0167-4838(02)00317-5

71. Kaya A, Mariotti M, Gladyshev VN. Cytochrome *c* peroxidase facilitates the beneficial use of H_2O_2 in prokaryotes. Proceedings of the National Academy of Sciences. 2017;114: 8678–8680. doi:10.1073/pnas.1710943114

72. Perkins A, Nelson KJ, Parsonage D, Poole LB, Karplus PA. Peroxiredoxins: Guardians Against Oxidative Stress and Modulators of Peroxide Signaling. Trends in biochemical sciences. 2015;40: 435–445. doi:10.1016/j.tibs.2015.05.001

73. Rhee SG. Overview on Peroxiredoxin. Molecules and Cells. 2016;39: 1–5. doi:10.14348/molcells.2016.2368

74. Lelandais G, Scheiber I, Paz-Yepes J, Lozano J-C, Botebol H, Pilátová J, et al. Ostreococcus tauri is a new model green alga for studying iron metabolism in eukaryotic phytoplankton. BMC Genomics. 2016;17: 319. doi:10.1186/s12864-016-2666-6

75. Vanlerberghe GC. Alternative Oxidase: A Mitochondrial Respiratory Pathway to Maintain Metabolic and Signaling Homeostasis during Abiotic and Biotic Stress in Plants. International Journal of Molecular Sciences. 2013;14: 6805–6847. doi:10.3390/ijms14046805

76. Gleason C, Huang S, Thatcher LF, Foley RC, Anderson CR, Carroll AJ, et al. Mitochondrial complex II has a key role in mitochondrial-derived reactive oxygen species influence on plant stress gene regulation and defense. Proceedings of the National Academy of Sciences of the United States of America. 2011;108: 10768–10773. doi:10.1073/pnas.1016060108

77. He J, Duan Y, Hua D, Fan G, Wang L, Liu Y, et al. DEXH box RNA helicase-mediated mitochondrial reactive oxygen species production in Arabidopsis mediates crosstalk between abscisic acid and auxin signaling. The Plant Cell. 2012;24: 1815–1833. doi:10.1105/tpc.112.098707

78. Pospíšil P. Production of Reactive Oxygen Species by Photosystem II as a Response to Light and Temperature Stress. Frontiers in Plant Science. 2016;7. doi:10.3389/fpls.2016.01950

79. Kimura M, Umemoto Y, Kawano T. Hydrogen peroxide-independent generation of superoxide by plant peroxidase: Hypotheses and supportive data employing ferrous ion as a model stimulus. Frontiers in Plant Science. 2014;5. doi:10.3389/fpls.2014.00285

80. Cárdenas-Monroy CA, Pohlmann T, Piñón-Zárate G, Matus-Ortega G, Guerra G, Feldbrügge M, et al. The mitochondrial alternative oxidase Aox1 is needed to cope with respiratory stress

but dispensable for pathogenic development in Ustilago maydis. PLoS ONE. 2017;12. doi:10.1371/journal.pone.0173389

81. Murik O, Tirichine L, Prihoda J, Thomas Y, Araújo WL, Allen AE, et al. Downregulation of mitochondrial alternative oxidase affects chloroplast function, redox status and stress response in a marine diatom. New Phytologist. 2019;221: 1303–1316. doi:10.1111/nph.15479

82. Popov VN, Simonian RA, Skulachev VP, Starkov AA. Inhibition of the alternative oxidase stimulates H2O2 production in plant mitochondria. FEBS Letters. 1997;415: 87–90. doi:10.1016/S0014-5793(97)01099-5

83. Kumari A, Pathak PK, Bulle M, Igamberdiev AU, Gupta KJ. Alternative oxidase is an important player in the regulation of nitric oxide levels under normoxic and hypoxic conditions in plants. Journal of Experimental Botany. 2019;70: 4345–4354. doi:10.1093/jxb/erz160

84. McDonald AE, Amirsadeghi S, Vanlerberghe GC. Prokaryotic orthologues of mitochondrial alternative oxidase and plastid terminal oxidase. Plant Molecular Biology. 2003;53: 865–876. doi:10.1023/B:PLAN.0000023669.79465.d2

85. Foresi N, Correa-Aragunde N, Parisi G, Caló G, Salerno G, Lamattina L. Characterization of a Nitric Oxide Synthase from the Plant Kingdom: NO Generation from the Green Alga Ostreococcus tauri Is Light Irradiance and Growth Phase Dependent. The Plant Cell. 2010;22: 3816–3830. doi:10.1105/tpc.109.073510

86. Astier J, Jeandroz S, Wendehenne D. Nitric oxide synthase in plants: The surprise from algae. Plant Science. 2018;268: 64–66. doi:10.1016/j.plantsci.2017.12.008

87. Hänsch R, Lang C, Riebeseel E, Lindigkeit R, Gessler A, Rennenberg H, et al. Plant Sulfite Oxidase as Novel Producer of H2O2 COMBINATION OF ENZYME CATALYSIS WITH A SUBSEQUENT NON-ENZYMATIC REACTION STEP. Journal of Biological Chemistry. 2006;281: 6884–6888. doi:10.1074/jbc.M513054200

88. Bauwe H, Hagemann M, Fernie AR. Photorespiration: Players, partners and origin. Trends in Plant Science. 2010;15: 330–336. doi:10.1016/j.tplants.2010.03.006

89. Bhagavan NV, Ha C-E. Chapter 25 - Nucleotide Metabolism. In: Bhagavan NV, Ha C-E, editors. Essentials of Medical Biochemistry. San Diego: Academic Press; 2011. pp. 333–354. doi:10.1016/B978-0-12-095461-2.00025-4

90. Godber BL, Doel JJ, Sapkota GP, Blake DR, Stevens CR, Eisenthal R, et al. Reduction of nitrite to nitric oxide catalyzed by xanthine oxidoreductase. The Journal of Biological Chemistry. 2000;275: 7757–7763. doi:10.1074/jbc.275.11.7757

91. Yesbergenova Z, Yang G, Oron E, Soffer D, Fluhr R, Sagi M. The plant Mo-hydroxylases aldehyde oxidase and xanthine dehydrogenase have distinct reactive oxygen species signatures and are induced by drought and abscisic acid. The Plant Journal. 2005;42: 862–876. doi:10.1111/j.1365-313X.2005.02422.x

92. Kundu TK, Velayutham M, Zweier JL. Aldehyde Oxidase Functions as a Superoxide Generating NADH Oxidase: An Important Redox Regulated Pathway of Cellular Oxygen Radical Formation. Biochemistry. 2012;51: 2930–2939. doi:10.1021/bi3000879

93. Mas A, Jamshidi S, Lagadeuc Y, Eveillard D, Vandenkoornhuyse P. Beyond the Black Queen Hypothesis. The ISME Journal. 2016;10: 2085–2091. doi:10.1038/ismej.2016.22

94. Fleury K. Reactive Oxygen Detoxification Genes in Phytoplankton. PhD thesis, Mount Allison University. 2019.

95. Kanehisa M, Furumichi M, Tanabe M, Sato Y, Morishima K. KEGG: New perspectives on genomes, pathways, diseases and drugs. Nucleic Acids Research. 2017;45: D353–D361. doi:10.1093/nar/gkw1092

96. Kanehisa M, Sato Y, Furumichi M, Morishima K, Tanabe M. New approach for understanding genome variations in KEGG. Nucleic Acids Research. 2019;47: D590–D595. doi:10.1093/nar/gky962

97. Kanehisa M. Toward understanding the origin and evolution of cellular organisms. Protein Science: A Publication of the Protein Society. 2019;28: 1947–1951. doi:10.1002/pro.3715

98. Nordberg H, Cantor M, Dusheyko S, Hua S, Poliakov A, Shabalov I, et al. The genome portal of the Department of Energy Joint Genome Institute: 2014 updates. Nucleic Acids Research. 2014;42: D26–31. doi:10.1093/nar/gkt1069

99. Vandepoele K, Van Bel M, Richard G, Van Landeghem S, Verhelst B, Moreau H, et al. Pico-PLAZA, a genome database of microbial photosynthetic eukaryotes. Environmental Microbiology. 2013;15: 2147–2153. doi:10.1111/1462-2920.12174

100. Kitts PA, Church DM, Thibaud-Nissen F, Choi J, Hem V, Sapojnikov V, et al. Assembly: A resource for assembled genomes at NCBI. Nucleic Acids Research. 2016;44: D73–D80. doi:10.1093/nar/gkv1226

101. Keeling PJ, Burki F, Wilcox HM, Allam B, Allen EE, Amaral-Zettler LA, et al. The Marine Microbial Eukaryote Transcriptome Sequencing Project (MMETSP): Illuminating the Functional Diversity of Eukaryotic Life in the Oceans through Transcriptome Sequencing. PLOS Biology. 2014;12: e1001889. doi:10.1371/journal.pbio.1001889

102. Leinonen R, Akhtar R, Birney E, Bower L, Cerdeno-Tárraga A, Cheng Y, et al. The European Nucleotide Archive. Nucleic Acids Research. 2011;39: D28–D31. doi:10.1093/nar/gkq967

103. Youens-Clark K, Bomhoff M, Ponsero AJ, Wood-Charlson EM, Lynch J, Choi I, et al. iMicrobe: Tools and data-dreaiven discovery platform for the microbiome sciences. GigaScience. 2019;8. doi:10.1093/gigascience/giz083

104. Liew YJ, Aranda M, Voolstra CR. Reefgenomics.Org - a repository for marine genomics data. Database. 2016;2016. doi:10.1093/database/baw152

105. Matasci N, Hung L-H, Yan Z, Carpenter EJ, Wickett NJ, Mirarab S, et al. Data access for the 1,000 Plants (1KP) project. GigaScience. 2014;3: 17. doi:10.1186/2047-217X-3-17

106. Los Alamos National Laboratory UD of E. Greenhouse. https://greenhouse.lanl.gov/greenhouse/organisms/; 2014.

107. Johnson M, Zaretskaya I, Raytselis Y, Merezhuk Y, McGinnis S, Madden TL. NCBI BLAST: A better web interface. Nucleic Acids Research. 2008;36: W5–W9. doi:10.1093/nar/gkn201

108. Wickham H. Tidyverse: Easily Install and Load the 'Tidyverse'. 2017.

109. Wickham H. Ggplot2: Elegant Graphics for Data Analysis. Springer-Verlag New York; 2016.

110. Wilke CO. Cowplot: Streamlined Plot Theme and Plot Annotations for 'ggplot2'. 2019.

111. Robinson D, Hayes A. Broom: Convert Statistical Analysis Objects into Tidy Tibbles. 2019.

112. Bache SM, Wickham H. Magrittr: A Forward-Pipe Operator for R. 2014.

113. Wickham H, François R, Henry L, Müller K. Dplyr: A Grammar of Data Manipulation. 2018.

114. Kassambara A. Ggpubr: 'Ggplot2' Based Publication Ready Plots. 2018.

115. Hester J. Glue: Interpreted String Literals. 2018.

116. Zhu H. kableExtra: Construct Complex Table with 'kable' and Pipe Syntax. 2019.

117. Fong Y, Huang Y, Gilbert P, Permar S. Chngpt: Threshold regression model estimation and inference. BMC Bioinformatics. 2017;DOI:10.1186/s12859-017-1863-x.

118. Mangiafico S. Rcompanion: Functions to Support Extension Education Program Evaluation. 2020.

119. Wei T, Simko V. R package "corrplot": Visualization of a Correlation Matrix. 2017.

120. Tang Y, Horikoshi M, Li W. Ggfortify: Unified Interface to Visualize Statistical Result of Popular R Packages. The R Journal. 2016;8: 478–489.

121. Horikoshi M, Tang Y. Ggfortify: Data Visualization Tools for Statistical Analysis Results. 2018.

122. Warnes GR, Bolker B, Lumley T, Johnson R. Gmodels: Various R Programming Tools for Model Fitting. 2018.

123. Warton DI, Duursma RA, Falster DS, Taskinen S. Smatr 3 - an R package for estimation and inference about allometric lines. Methods in Ecology and Evolution. 2012;3: 257–259.

124. Aust F. Citr: 'RStudio' Add-in to Insert Markdown Citations. 2018.

125. Xie Y. Knitr: A Comprehensive Tool for Reproducible Research in R. In: Stodden V, Leisch F, Peng RD, editors. Implementing Reproducible Computational Research. Chapman and Hall/CRC; 2014.

126. Xie Y. Dynamic Documents with R and knitr. Second. Boca Raton, Florida: Chapman and Hall/CRC; 2015.

127. Xie Y. Knitr: A General-Purpose Package for Dynamic Report Generation in R. 2018.

128. Xie Y. Bookdown: Authoring books and technical documents with R markdown. 2019.

129. Cooper GM. The Complexity of Eukaryotic Genomes. The Cell: A Molecular Approach 2nd edition. 2000.

130. Bienert GP, Schjoerring JK, Jahn TP. Membrane transport of hydrogen peroxide. Biochimica et Biophysica Acta (BBA) - Biomembranes. 2006;1758: 994–1003. doi:10.1016/j.bbamem.2006.02.015

131. Diaz JM, Plummer S. Production of extracellular reactive oxygen species by phytoplankton: Past and future directions. Journal of Plankton Research. 2018;40: 655–666. doi:10.1093/plankt/fby039

132. Wheeler G, Ishikawa T, Pornsaksit V, Smirnoff N. Evolution of alternative biosynthetic pathways for vitamin C following plastid acquisition in photosynthetic eukaryotes. eLife. 4. doi:10.7554/eLife.06369

133. CCMP2712 | NCMA - Culturing Diversity. https://ncma.bigelow.org/ccmp2712#.Xpnx-VNKg6W;

134. CCMP1102 | NCMA - Culturing Diversity. https://ncma.bigelow.org/ccmp1102#.XpnIoVNKg6U;

135. D'Alelio D, Amato A, Luedeking A, Montresor M. Sexual and vegetative phases in the planktonic diatom Pseudo-nitzschia multistriata. Harmful Algae. 2009;8: 225–232. doi:10.1016/j.hal.2008.05.004

136. Martino AD, Meichenin A, Shi J, Pan K, Bowler C. Genetic and phenotypic characterization of *Phaeodactylum Tricornutum* (Bacillariophyceae) accessions1. Journal of Phycology. 2007;43: 992–1009. doi:10.1111/j.1529-8817.2007.00384.x

137. Orlova TY, Stonik IV, Aizdaicher NA, Bates SS, Léger C, Fehling J. Toxicity, morphology and distribution of *Pseudo-Nitzschia Calliantha*, *P. Multistriata* and *P. Multiseries (Bacillariophyta)* from the northwestern Sea of Japan. Botanica Marina. 2008;51. doi:10.1515/BOT.2008.035

138. Matsumoto M, Mayama S, Nemoto M, Fukuda Y, Muto M, Yoshino T, et al. Morphological and molecular phylogenetic analysis of the high triglyceride-producing marine diatom, *Fistulifera Solaris Sp. Nov. (Bacillariophyceae)*. Phycological Research. 2014;62: 257–268. doi:10.1111/pre.12066

139. Harris A, Medlin L, Lewis J, Jones K. *Thalassiosira* species (Bacillariophyceae) from a Scottish sea-loch. European Journal of Phycology. 1995;30: 117–131. doi:10.1080/09670269500650881

140. Bo W, Baihui C, Qi L, Quanxi W. Morphological description of the Genus *Skeletonema (Bacillariophyceae)* in Yangtze River Estuary, China. Journal of Shanghai Normal University(Natural Sciences). 2013;42: 6.

141. CCMP2513 | NCMA - Culturing Diversity. https://ncma.bigelow.org/ccmp2513#.Xp-e2FNKiqR;

142. Nitzschia palea | Species - Diatoms of North America. https://diatoms.org/species/nitzschia_palea;

143. EOS - Phytoplankton Encyclopedia Project Leptocylindrus danicus. Leptocylindrus danicus. https://www.eoas.ubc.ca/research/phytoplankton/diatoms/centric/leptocylindrus/l_danicus.html;

144. CCMP982 | NCMA - Culturing Diversity. https://ncma.bigelow.org/ccmp982#.Xp-gCVNKhQJ;

145. EOS - Phytoplankton Encyclopedia Project Chaetoceros debilis. Chaetoceros debilis. https://www.eoas.ubc.ca/research/phytoplankton/diatoms/centric/chaetoceros/c_debilis.html;

146. CCMP3096 | NCMA - Culturing Diversity. https://ncma.bigelow.org/ccmp3096#.Xp-gq1NKhQJ;

147. CCMP1317 | NCMA - Culturing Diversity. https://ncma.bigelow.org/ccmp1317#.Xp-gzlNKhQJ;

148. CCMP1010 | NCMA - Culturing Diversity. https://ncma.bigelow.org/ccmp1010#.Xp-hA1NKhQJ;

149. Hoppenrath M, Beszteri B, Drebes G, Halliger H, Beusekom JEEV, Janisch S, et al. Thalassiosira species (Bacillariophyceae, Thalassiosirales) in the North Sea at Helgoland (German Bight) and Sylt (North Frisian Wadden Sea) a first approach to assessing diversity. European Journal of Phycology. 2007;42: 271–288. doi:10.1080/09670260701352288

150. EOS - Phytoplankton Encyclopedia Project Ditylum brightwellii. Ditylum brightwellii. https://www.eoas.ubc.ca/research/phytoplankton/diatoms/centric/ditylum/d_brightwellii.html;

151. Chaetoceros curvisetus P.T. Cleve, 1889 | Nordic Microalgae. http://nordicmicroalgae.org/taxon/Chaetoceros%20curvisetus;

152. CCMP2467 | NCMA - Culturing Diversity. https://ncma.bigelow.org/ccmp2467#.Xp-h9lNKhQJ;

153. CCMP332 | NCMA - Culturing Diversity. https://ncma.bigelow.org/ccmp332#.Xp-iMFNKhQI;

154. CCMP2468 | NCMA - Culturing Diversity. https://ncma.bigelow.org/ccmp2468#.Xp-jElNKhQK;

155. Lajeunesse TC, Parkinson JE, Reimer JD. A genetics-based description of *Symbiodinium Minutum* sp. Nov. And *S. Psygmophilum* sp. Nov. (Dinophyceae), two dinoflagellates symbiotic with cnidaria. Journal of Phycology. 2012;48: 1380–1391. doi:10.1111/j.1529-8817.2012.01217.x

156. Lee SY, Jeong HJ, Kang NS, Jang TY, Jang SH, Lajeunesse TC. *Symbiodinium Tridacnidorum* sp. Nov., a dinoflagellate common to Indo-Pacific giant clams, and a revised morphological description of *Symbiodinium Microadriaticum* Freudenthal, emended Trench & Blank. European Journal of Phycology. 2015;50: 155–172. doi:10.1080/09670262.2015.1018336

157. Chen W-NU, Hsiao Y-J, Mayfield AB, Young R, Hsu L-L, Peng S-E. Transmission of a heterologous clade C *Symbiodinium* in a model anemone infection system via asexual reproduction. PeerJ. 2016;4. doi:10.7717/peerj.2358

158. CCMP1383 | NCMA - Culturing Diversity. https://ncma.bigelow.org/ccmp1383#.Xp-jmlNKhQJ;

159. CCMP2088 | NCMA - Culturing Diversity. https://ncma.bigelow.org/ccmp2088#.Xp-jzVNKgUt;

160. CCMP1779 | NCMA - Culturing Diversity. https://ncma.bigelow.org/ccmp1779#.Xp-j8VNKhQJ;

161. CCMP526 | NCMA - Culturing Diversity. https://ncma.bigelow.org/ccmp526#.Xp-kUFNKhQL;

162. CCMP1776 | NCMA - Culturing Diversity. https://ncma.bigelow.org/ccmp1776#.Xp-kqlNKhQJ;

163. Roscoff Culture Collection | Marine Microalgae, Macroalgae, Protists, Bacteria and Viruses RCC1115. RCC1115. http://roscoff-culture-collection.org/rcc-strain-details/1115;

164. Roscoff Culture Collection | Marine Microalgae, Macroalgae, Protists, Bacteria and Viruses RCC745. RCC745. http://roscoff-culture-collection.org/rcc-strain-details/745;

165. Roscoff Culture Collection | Marine Microalgae, Macroalgae, Protists, Bacteria and Viruses RCC4221. RCC4221. http://roscoff-culture-collection.org/rcc-strain-details/4221;

166. Roscoff Culture Collection | Marine Microalgae, Macroalgae, Protists, Bacteria and Viruses RCC809. RCC809. http://roscoff-culture-collection.org/rcc-strain-details/809;

167. Moreau H, Verhelst B, Couloux A, Derelle E, Rombauts S, Grimsley N, et al. Gene functionalities and genome structure in *Bathycoccus Prasinos* reflect cellular specializations at the base of the green lineage. Genome Biology. 2012;13: R74. doi:10.1186/gb-2012-13-8-r74

168. CCMP1545 | NCMA - Culturing Diversity. https://ncma.bigelow.org/ccmp1545#.Xp-mqFNKhQJ;

169. Waltman PH, Guo J, Reistetter EN, Purvine S, Ansong CK, van Baren MJ, et al. Identifying Aspects of the Post-Transcriptional Program Governing the Proteome of the Green Alga *Micromonas Pusilla*. Mills K, editor. PLOS ONE. 2016;11: e0155839. doi:10.1371/journal.pone.0155839

170. Foflonker F, Price DC, Qiu H, Palenik B, Wang S, Bhattacharya D. Genome of the halotolerant green alga *Picochlorum Sp.* reveals strategies for thriving under fluctuating environmental conditions. Environmental Microbiology. 2015;17: 412–426. doi:10.1111/1462-2920.12541

171. Blanc G, Agarkova I, Grimwood J, Kuo A, Brueggeman A, Dunigan DD, et al. The genome of the polar eukaryotic microalga *Coccomyxa Subellipsoidea* reveals traits of cold adaptation. Genome Biology. 2012;13: R39. doi:10.1186/gb-2012-13-5-r39

172. Hagino K, Bendif EM, Young JR, Kogame K, Probert I, Takano Y, et al. New evidence for morphological and genetic variation in the cosmopolitan coccolithophore *Emiliania Huxleyi*(Prymnesiophyceae) from the COX1b-ATP4 genes. Journal of Phycology. 2011;47: 1164–1176. doi:10.1111/j.1529-8817.2011.01053.x

173. Lizzul AM, Lekuona-Amundarain A, Purton S, Campos LC. Characterization of *Chlorella Sorokiniana*, UTEX 1230. Biology. 2018;7. doi:10.3390/biology7020025

174. van den Hoff J, Ferris JM. Pleomorphism in the Antarctic flagellate *Pyramimonas Gelidicola* (Prasinophyceae, Chlorophyta). Polar Research. 2009;28: 426–432. doi:10.1111/j.1751-8369.2009.00123.x

175. Harris EH. Chlamydomonas as a Model Organism. Annual Review of Plant Physiology and Plant Molecular Biology. 2001;52: 363–406. doi:10.1146/annurev.arplant.52.1.363

176. Heimann K, Huerlimann R. Chapter 3 - Microalgal Classification: Major Classes and Genera of Commercial Microalgal Species. In: Kim S-K, editor. Handbook of Marine Microalgae. Boston: Academic Press; 2015. pp. 25–41. doi:10.1016/B978-0-12-800776-1.00003-0

177. CCMP1897 | NCMA - Culturing Diversity. https://ncma.bigelow.org/ccmp1897#.Xp-nK1NKhQJ;

178. CCMP291 | NCMA - Culturing Diversity. https://ncma.bigelow.org/ccmp291#.Xp-npFNKhQI;

179. CCMP1516 | NCMA - Culturing Diversity. https://ncma.bigelow.org/ccmp1516#.Xp-n9FNKhQI;

180. CCMP2436 | NCMA - Culturing Diversity. https://ncma.bigelow.org/ccmp2436#.Xp-oeVNKhQI;

181. Bendif EM, Probert I, Schroeder DC, de Vargas C. On the description of *Tisochrysis Lutea* gen. Nov. Sp. Nov. And *Isochrysis Nuda* sp. Nov. In the Isochrysidales, and the transfer of Dicrateria to the Prymnesiales (Haptophyta). Journal of Applied Phycology. 2013;25: 1763–1776. doi:10.1007/s10811-013-0037-0

182. CCMP2298 | NCMA - Culturing Diversity. https://ncma.bigelow.org/ccmp2298#.Xp-onFNKhQJ;

183. CCMP1984 | NCMA - Culturing Diversity. https://ncma.bigelow.org/ccmp1984#.Xp-o3VNKhQI;

184. CCMP2097 | NCMA - Culturing Diversity. https://ncma.bigelow.org/ccmp2097#.Xp-pClNKhQJ;

185. CCMP1429 | NCMA - Culturing Diversity. https://ncma.bigelow.org/ccmp1429#.Xp-pNFNKhQJ;

186. CCMP1756 | NCMA - Culturing Diversity. https://ncma.bigelow.org/ccmp1756#.Xp-pZ1NKhQJ;

187. CCMP1328 | NCMA - Culturing Diversity. https://ncma.bigelow.org/ccmp1328#.Xp-pqFNKhQJ;

188. Peperzak L, Colijn F, Vrieling EG, Gieskes WWC, Peeters JCH. Observations of flagellates in colonies of Phaeocystis globosa (Prymnesiophyceae); a hypothesis for their position in the life cycle. Journal of Plankton Research. 2000;22: 2181–2203. doi:10.1093/plankt/22.12.2181

189. Wang X, Wang Y, Smith WO. The role of nitrogen on the growth and colony development of Phaeocystis globose (Prymnesiophyceae). European Journal of Phycology. 2011;46: 305–314. doi:10.1080/09670262.2011.602430

189. Team RC. R: A Language and Environment for Statistical Computing. R Foundation for Statistical Computing; 2019.

190. Wehr JD, Sheath RG. Freshwater Algae of North America. A volume in Aquatic Ecology. 2003; doi:10.1016/b978-0-12-741550-5.x5000-4

191. Feilke K, Yu Q, Beyer P, Sétif P, Krieger-Liszkay A. In vitro analysis of the plastid terminal oxidase in photosynthetic electron transport. Biochimica et Biophysica Acta (BBA) - Bioenergetics. 2014;1837: 1684–1690. doi:10.1016/j.bbabio.2014.07.016

192. Krieger-Liszkay A, Feilke K. The Dual Role of the Plastid Terminal Oxidase PTOX: Between a Protective and a Pro-oxidant Function. Frontiers in Plant Science. 2016;6. doi:10.3389/fpls.2015.01147

193. Nawrocki WJ, Tourasse NJ, Taly A, Rappaport F, Wollman F-A. The Plastid Terminal Oxidase: Its Elusive Function Points to Multiple Contributions to Plastid Physiology. Annual Review of Plant Biology. 2015;66: 49–74. doi:10.1146/annurev-arplant-043014-114744

194. Information on EC 1.8.3.1 - sulfite oxidase. BRENDA. Available: https://www.brenda-enzymes.org/enzyme.php?ecno=1.8.3.1

195. Information on EC 1.1.3.15 - (S)-2-hydroxy-acid oxidase. BRENDA. Available: https://www.brenda-enzymes.org/enzyme.php?ecno=1.1.3.15

196. Radi R. Oxygen radicals, nitric oxide, and peroxynitrite: Redox pathways in molecular medicine. Proceedings of the National Academy of Sciences of the United States of America. National Academy of Sciences; 2018. Available: https://www.ncbi.nlm.nih.gov/pmc/articles/PMC6003358/

197. Information on EC 1.17.3.2 - xanthine oxidase. BRENDA. Available: https://www.brenda-enzymes.org/enzyme.php?ecno=1.17.3.2

198. Information on EC 1.2.3.1 - aldehyde oxidase. BRENDA. Available: https://www.brenda-enzymes.org/enzyme.php?ecno=1.2.3.1

199. Xu J, Fan X, Zhang X, Xu D, Mou S, Cao S, et al. Evidence of coexistence of C_3 and C_4 photosynthetic pathways in a green-tide-forming alga, Ulva prolifera. PloS one. Public Library of Science; 2012. Available: https://www.ncbi.nlm.nih.gov/pmc/articles/PMC3353924/

200. Roberts K, Granum E, Leegood RC, Raven JA. C3 and C4 pathways of photosynthetic carbon assimilation in marine diatoms are under genetic, not environmental, control. Plant physiology. American Society of Plant Biologists; 2007. Available: https://www.ncbi.nlm.nih.gov/pmc/articles/PMC1976569/

201. Wang C, Guo L, Li Y, Wang Z. Systematic comparison of C3 and C4 plants based on metabolic network analysis. BMC systems biology. BioMed Central; 2012. Available: https://www.ncbi.nlm.nih.gov/pmc/articles/PMC3521184/

202. Foyer CH. Reactive oxygen species, oxidative signaling and the regulation of photosynthesis. Environmental and Experimental Botany. Elsevier; 2018. Available: https://www.sciencedirect.com/science/article/pii/S0098847218305495

203. Vass I. Role of charge recombination processes in photodamage and photoprotection of the photosystem II complex. Physiologia Plantarum. 2011;142: 6–16. doi:10.1111/j.1399-3054.2011.01454.x

Appendices

Appendix 1

Probes for ROS Production enzymes

>tps:THAPSDRAFT_42992 no KO assigned | (RefSeq) AOX2; mitochondrial alternative oxidase (A)

MFTKTHGKYTKEELDIKMTHVEPESALDRLALFAVKVTRFGFDQATGWNRGSITTDKVLNRAIFLETVAAI
PGMVAAIIRHFRSLRNMARDGGMLNMFLEEANNERMHLLTFIRMKDPGYLFRGAVVGSQFAFGSAFLVLY
MISPAFCHRFVGYIEEEACATYTKIIKAIEEAPEGSDLAKWRTEEAPKIAKGYWHLGEEGTVLDVMRAVRA
DEAEHRDVNHAVSGVAHDTVNPLYDPREKMDSMMKRYVKDMMERSETKTATS

>ota:OT_ostta09g00050 no KO assigned | (RefSeq) Alternative oxidase (A)

MDGSARRARAHSRAPGAPLASARSFASSAEQPAPKEDEATEVANVKRLDDPPRGASQGSYMLFHPMYDLR
QVENVKPAHRKPKWASDYLAYGLVQITRWGFDKVTGYSPKKALSTDQWLARFIFLETVAGVPGMVGAM
LRHMMSLRTLKRDHGWIHTLLEEAENERMHLLTFLKLREPGLMFRLAVLAAQGVFFNAFFLSYLISPRVCH
RFVGYLEEEAVRTYTHALHDIDGDGQASEWARKPAPMLAIKYWRMPEDATVRDLIIAVRADEASHSHVN
HTLSSMGIRQANPFHVGHTELPENFVDPPPGFVPEHCR

>bpg:Bathy15g01150 no KO assigned | (RefSeq) alternative oxidase (A)

MCAACRRAAGLLLKQRPSSSSYTSSSTSIFSRTHRIVDGKTDVFRSAAISGTSSTMHARTRCTFHTNAKNEEE
HQDSMKRMSKTRNFHSTSFAAGGVSTHKRAEKKRFSAEAATTSTEEEMGETDVRAKKDETKMKKSAQSY
MLAHPTYDFGFIEQLKPKHRPPQGARDYVSMFAVWSARKGFDTITSYSHEKSLTKDQWLFRFIFLETVAGIP
GMVAGMLRHMNSLRLLRHDNGWIHTLLEEAENERMHLMTFLNMKQPSIFFRAGVLAAQGVFFNAFFFSY
LISPRTCHRFVGYLEEEAVRTYTHALNDIDSGGTDARQWAKERAPKLAIEYWKMDEDATIRDVLLAVRAD
EASHAHVNHTFSSMGTTQKNPFVKGESHLPENFVEPPPGFVPSEENRVAKDADSF

>ota:OT_ostta02g02300 no KO assigned | (RefSeq) Nitric oxide synthase, oxygenase domain (A)

TGMFDALPIVVQINPETPPAMFTLPDQCFLEVPIRHPTIRGISQLGLKWYGIPAVSNITMDLGGLHYTAAPFN
GWYMVTEIATRNFGDESRYNLLPQIAEAMGLDTSTHDTLWRDHALAAINYAVFDSFKGALTKSCMQRQV
RNAMAIQRVIEICTL

>tps:THAPSDRAFT_25299 K10534 nitrate reductase (NAD(P)H) [EC:1.7.1.1 1.7.1.2 1.7.1.3] | (RefSeq) predicted protein (A)

MAPINGMKRADTSESSVDLTTLIKPSTSIQNFKSISSSQPTKEQTCVDLYGPYPSSIPVPTISKDGSVPPTDVTS
KAKTMWDVQSYPDHRDVGTPDEWIPRDGKLVRLTGRHPFNVEPPLSVHQEHKFITPTCLHYVRNHGACPN
IKWEEHRVRVGGLVDTPLDLGMDEIVAMEPRELPVTLVCAGNRRKEQNMIRQTIGFNWGAGGVSTNVWK
GVTLRDLLLKAGVSEKNMAGKHVEFIGAEDLPNKVGPGPFKDEPWGKLVKYGTSVPLARAMNPAYDILIA
YEANGEVLQPDHGYPIRLIIPGYIGGRMIKWLTDINVLEHETKNHYHYHDNRILPPHITAEESLTGGWWYKP
EYIFNELNINSAMTAPDHNETIDLASSIGSSYEVGGYAYTGGGRRISRVEVSTDGGVHWEIANINQIEKPTDY
GMYWCWIWWTFDLKVADLVGTKELWCRAWDESNNVQPNDPTWNLMGMGNNQVFRIKVHLDKDVNGK
HVFRFEHPTKPGQQEGGWMTTLAGKPDSAGFGRLLEQGQPAKEAAPAAAPAKTSGSKLIKMEEVRKHNK
EEDVWIVVNNKVYDCTEYLDLHPGGADSILINAGEDATEDFVAIHSTKATKMLDKFYVGDLDTTSVAVVS
DAEEERLCPKTGRKVALDPKHKHAFKLQTKTVLSRDSFELDFALQTPEHVLGLPTGKHVFLSADINGEMV
MRRYTPTTSDHDIGQIKFVIKAYPPCERFPLGGKMSQYLDSLKVGDTIDMRGPVGEFDYHGNGKFLKEHDE
CYATHFNMIAGGTGITPVMQIASEILRNPDDKTTMSLVFGCREEGDLLLRSTLDEWAVKHADRFKVHYVLS
ENAPPGWTHSIGFVSKELFEKELFPAGDNCYNLMCGPPIMLERGCTPNLKALGHKEDNIFSF

>aaf:AURANDRAFT_55689 K10534 nitrate reductase (NAD(P)H) [EC:1.7.1.1 1.7.1.2 1.7.1.3] | (RefSeq) hypothetical protein (A)

MGPARADAGFKRHPEEFPVPDPKDASTPDAWVKRNPALVRLTGRHPFNVEPPLPLLEAHGHSTPASLHYV
RNHGAVPVAYGSAAEADAVYDGWRCEVLAGGGVEAKSLSMADLEKFPKVVVPSLLVCAGNRRKEQNMI

KRTIGFNWGAAGLGMSEWGGCHLADVLASLGAPTDPAAWDGGGHVCFRGPDKELPGGADGSYGTSLTL
RYVMDKSNDVILAWDCQNGARLQADHGFPLRILIPGFIGGRMVKWLKEIKISPEQSDNHYHFKDNRVLPV
NVTPEQAEAEGWWFKPDYIINELNINSAMFHPGHGEVLDLATAGPTYDVEGYAYGGGGRKIIRVEVTLDG
GASWFLVKDGDVTHPPNTPNKAGKYWGWCFWKITVPTADLLKAPNVACRAWDAAMNTQPSNLTWNVM
GMLNNPWFTVVKHFDAGPAGTPVLVFEHPTLAGAQAGGWMTDDARRLAGASLTPESAGAAAMRDMHA
ARAAAATGAPLGNTYTLADVAKHDTPQDCWIAVNGVVYDTNPYLAEHPGGASSITMNAGTDATDEFTAI
HSRKAWTLLDKYAIGTL

>tps:THAPSDRAFT_406 K11517 (S)-2-hydroxy-acid oxidase [EC:1.1.3.15] | (RefSeq) GOX; glycolate oxidase (A)

MHVKICNAGDYQRVARSILPTPLYEYLASGTDDEQTLSENESAFKAWYLRPRVMRPVGSISTVTTLFGQRL
SMPVFVSPAGVHALCDEVHGECAAARACGKVGTIFGLSQHATRSIEQVAEATQGNTNLWYQSYILKDREM
TLRLARRAAKAGYRGIFLTVDSVRFGFREADARNNFSSLPEPHRLVNYDDEVSQAQHPKKAWVAPEASVD
KSKIYSGQEEAWDQNTEQLFEQNPSWEDVRWLKREVCRDLPLIVKGIMTAEDAIEAKKAGADGVMVSNH
GGRGLDSALPTIDVLPEIVAAVGDQFPVLLDSGIRRGTDVLKALALGATAVGIGKPLFFALSVGGEDAVLNL
LQMFQRETEAAMAICGCKSVSDVTRQLVTRHPSGSGRVGKYERSKL

>mis:MICPUN_98069 no KO assigned | (RefSeq) GOX2; glycolate oxidase (A)

MVFDYLDAGADDEITIRRNKDAYSQLELHYRILAGLSPPLDMSTRVMGRDVKIPFFVSPTAGSKMFHADGE
VGVARAASAAGAMYSLSTMGTAAPAEVAPAVPAHHPKLFQLYVWKDRSLVRDMLAQARENGFHALALT
VDLTWYGNRERDHRNGFTVPPAYTAKQTWEAMRRPAWTWDFLSSPEYAYAAVAFIRDAFDPSFSWDDA
EWLCQEWNEGPVALKGVVRPSDALKAVDRGFDAVWVSNHGGRQLETAPAPIDVLPSIRDAMGGIVVDGG
VQRGTDVLKGLAMGADAVAIGKPYLYGLCAGGEAGVRKAFDVLTDELERAMGLLGVGTVRELRARMAA
GEELVRRRHPSPRDFPDRGALDRGYGGGVF

>mis:MICPUN_57273 K11517 (S)-2-hydroxy-acid oxidase [EC:1.1.3.15] | (RefSeq) GOX1; glycolate oxidase (A)

MAKEAVGKVDLDAIVCLDDMERAAQRVMDRQDFDYFAGGAETESTLRANRAAFSRVTIWPRCMVDVSD
VDTTTHVPALGLRNLAAPLLIAPVAMQRAAHPDGECAAARACAAHSIPYCASQQSTTAIEEIGRAGGDDAP
RMFQLYVLSDREATTRLIRRAESAGATALCITVDAPVLGRRERDVRNRFELKAGLKLANVDAKKNQNQNQ
NQAGPDKSAVDAKRAQSAIARRIGGRDASLTWDHLAWLRSVTHLPLVLKGIVTYADAARAAKEGVAGV
WVSNHGGRQLDGSPATLDALPEVVAGVKEGVKEGAPTCVVIFDGGVRRGTDALKALALGADLVAVGRPV
AWGLACGGELGVGKAVELLTEELRTAMTLAGCRDVRSARNRELVQVVGETPPRSRL

>tps:THAPSDRAFT_270071 K00106 xanthine dehydrogenase/oxidase [EC:1.17.1.4 1.17.3.2] | (RefSeq) hypothetical protein (A)

MHVCFRCWQRMDAMSLLLRVWGVKEDYLHPIQRAMVDMHGSQCGFCTPGIIMALYGLFAAEGSISQRQP
TVSHLEEHLDGNLCRCTGYRPIWDAARSLCVDDDVEEGGVEGPCGQHKQPDCENGGGDKLCCSSTGSKIR
DFQAVLEAKHSGAWWNQPNDMFPRELLEKGDDMQQLLSKPLLVVDTTIHNGGTWFQPTSLEELLDLFREF
GTDGGLKMVVGNTEVGIEMKFKHAIYPRLVHPMEAIHTLYEIFSTETHFHVGACSSLSMLQHVSDEVKKLL
AHRQSRTAKPMHDMLRWFASTQIRNVACLGGNLATASPISDMNPLLASMNGTIVLASRPRSDGAVVRRHI
PVSDFFVGYRTVEKSDLEVIERVDVPLVSKFEYVVPFKQARRREDDISIVTSGMRMKLSPAESGWIIDEIAIA
FGGMAPKTVMARATMEELTGKPFEEATFVQARSVLQKEFRMPEDVPGGQSEYRLTLACSFLHKFFLHCVG
ELKKDVETSSRDERFPTIPFLTTAAKNSDNPDAVGRSATHASGPLHCTGEAAYADDIPAPENLLHGSLILAS
KCHAPLASIDISPALRIPGVAAAFTHDDIVKLGGDNRMGPVILDDVAFLPIGEKVDFVGQVLGVVVAISQEIA
EKGARAVAVEYGDDEEGSAIVSIEDAIRAGSFWTDFRHEMKRGGDAEQILRQTQVDGKRLVVVEGSMRCG
GQEHFYLEPNSTLAIPSESATNLTIYCSTQAATKTQDFCARVTNTPAAKVVVRMKRMGGGFGGKETRSVFV
SVAAAVAAKLTNRPVRLTLNRDTDMSITGGRHAFLAHYKAGAIVQENGSVKLHALDVNLYNNGGCKFDL
TGPVLDRALFHVDNCYNWPNFHSVGTPCKTSQPPHTAFRGFGGPQGMIVSEHIMDHLAVECNISGDKLRRE
NMYTLQDCTPFGMRFGGEFTGKWNVPSMWDRLYDGLDVPGRRTATAEFNAKNKWTKRGIGFIPTKFGIA
FTAKFMNQGGALVHLYTDGTVLVTHGGTEMGQGLHTKVCQVAAQAFGIPLYDVYVNDSSTDKVANTLPS
AASMSTDLYGMATLDACKQIIKRIQPIREQLPPDAKLSEVAKKAFFERVDLSAHGFFAVDNDHLPENSWKG
HPFNYFTQGVAFAEVEIDVLSGDHKTLSVEVLVDVGSSINPAIDIGQIEGAFIQGMGWCTMEEVVYADDDH
TWIRPRARVFTTGPGTYKIPAFNDVPEKFNVSLLENADNPFAVHSSKAVGEPPFFLGCSVFYAIKDAVSAAR
GKKHPGYFEFRMPATSERIRMSCGDVIATECIEGETASFQPKGSF

>pti:PHATRDRAFT_15968 K00106 xanthine dehydrogenase/oxidase [EC:1.17.1.4 1.17.3.2] | (RefSeq) hypothetical protein (A)

NQTLLSFLRDVLRLTGSKLGCAEGGCGACTVMLSKKNVDTGKIKHFSVNACLMPVLAADGCHVTTVEGIG
TVKNDNLHPVQNAMVDMHGSQCGFCTPGIIVSIYALLANNPTTAYLEEHLDGNLCRCTGYRPIWDAARSL
CDDGEELVKGPCGTACRECPEREACDQDCNVQDKATSADNMCCSSSKDKMSTYKETFLTNKDSWRAQPN
VMFPKVLMDTASVESTLLTKPLMIVDRSEYHTGGTWFKPTTFAGLLALLQEFGGTGTGACKIVVGNTEVGI
ETRFKYAVYPRLISPSESIRELFGFEVSGANLIIGSCCPLSTIQHHCNALGEQDLLVRTVMPIHDMLRWFAST
QIRNVACLGGNLVTASPISDMNPMLASMGAKLVIASLDATDKTTICRRYVDVSDFFVKYRTVDLKPTEILE
RIEVPVLRNPFEYLKPFKQARRREDDISIVTSGMRLKLTVVDHEYIIEEASLAFGGMAPTTVLATETVKILIGS
AFCAKSFESATEALLQELSLPEAVPGGQAAFRMTLATSFLYKFFLSVVADLKADISAIRANPSAYPGMEVDL
PDPPSVDTMEESGTTTVVGKASAHQSGPLHCTGEAAYCDDIPMPAGTLQACLVLARECGGVFEAMDVAEA
LAIPGVIGIYNYDSLVGLGGSNELGPIIHDETVFLRPGDIVRTVGQVLGIAVAETLEAAEFAARTVHVTCSQP
KEKVVVTVEDAIETGSFYEFSRHSMERGDIAIIDSLATIADSTGTPSLGDVVKISGTFRSGAQEHFYLETNAA
LVIPSESDTNLTIYASTQAPTETQAYCASATGTPASKVVVRMKRMGGGFGGKETRSVFAACAAAVAAKCA
SRPIRLTLSRDVDMKITGTRHVFLSKYHASAQITENGAKLVAFDVKLFANGGSSFDLSGPVVDRALFHVDG
VYMFPSFRAEGVPCKTVQAPHTAFRGFGGPQGMAVVEHVMDHLALATNVDADKLRRMNMYNDGEATPF
GMIVGGHHSGNWNVPVMWDRLVQELDVPHRRERIAQFNAKHKWLKRGLCLIPTRFGIAFTTKFMNQGGA
LVHLYVDGTVLVTHGGTEMGQGLHTKVCQVAAQSFGIPLNDVYVNDTSTDKVANSLPTAASMSTDTYGM
ATLDACRQILKRLEPFREKLGADAPLKDVAHAAFFARVDLTAHGFFTVDDKRCGFDWKKERPEGFPDDKP
ANSWRGNPFNYFTQGVVCTEVEIDVLSGNHRTLQSDLLVDVGASINPAIDIGQIEGAFVQGMGWSTIEEVT
YADDDHTWIRPRGSLFTSGPGTYKIPAFNDVPETFNVSLMDNVDNPFAVHSSKAIGEPPFFLGASVFYAIKD
AVTAARSQNLGQTSYFEMRMPATSERIRMYCADPLASQAVS

>XP_005536398.1 plastid terminal oxidase [Cyanidioschyzon merolae strain 10D]

MTGFISTRAGVSSTWREPGRWQTIRSSRSGGRCYFRCRRQFHLWARRDAKAPGKSAAREPVSNSTGEANA
LKPPVPYGSMLERERKERPGSAGILGLRNFVRESRAIALDLYDKLRGIDESRRLPGALALTLDDAAVNEREK
RRDELTGYLSNAPWISRVPYEIACRFLDWAFTDRPIARFWFLETVARMPYFSYLSVLHLYETFNWLHLAEL
RRTHFAEEWNELHHLLIMSALGGDAKWSDRFLAYHLSIIYYWLLVVMYIVSPRLSYNFSELLEKHAVDTYE
QFLTENEHRLKALPAPAIAVRYYANEVAYTFQAFGDENGSAVETSRPPVQTLYDAFLNIRLDEEEHVRTME
ACQNYDLVERLTSSPYLREQSPEDGVPAHADKHAEESSADQTGSRAAWNRWADAVNQAGRRPGPDTRSE
DADQKP

>XP_005840480.1 plastid terminal oxidase [Guillardia theta CCMP2712]

MASMRFVLLFLMLISISDAFIGHGFAGVNLPLQRKAYSAHKSRGPIVKCNPEDSPVISENFDSMFRKDGTTW
GSKSYPVSTVEEPEPLDIVTKSIAQALVTVLKGSLDWYYHKKSDFARFFVLETVARVPYFAYMSVLHLYES
FGYHDRAHWIKIHYAEADNELHHLLIMEALGGNKEFSDRWIAQHAAFAYYWFCVTFYFLHPRGAYYVMS
LIENHAYHTYSKYIEANKSWLASQPSPAIAKEYYEGGDLYLFDAFHTTRAEEQERRPRVQSLLDTFESIRDD
ESQHHRTMLSLVERGRP

>XP_001703466.1 plastid terminal oxidase [Chlamydomonas reinhardtii]

MLAARQLSSHRPGRFGHRNRAALRIQAISAPVTTGEGECPLFQTREGKIVPAMCADYGFRSGSGRLYQEGY
GEVPKDVWQLAKDNYLHEFTQLRRSTRYPPSDITAPDGAVAKVLHSAGAAAAARAFGSLDKALENAGVLPE
LAPPPVLSALETQEFKQIRAKLDKLELSVSDVVAVEHARIARTGDMTSPAWVKAPFYALCFVLDVMYPKN
KAIEKFWVLETVARIPYFAYISILHLYESLGFWRAGAELRKIHFAEEWNEMHHLQIMESLGGDRAWFDRFIA
EHAAVFYYWVLIAFYLVSPRMAYNFMQRVELHAADTYSAFVERNRTALADIPPPLVALQYYYSDDLYLFD
EFQTASRGAPGVPPRRPPCENLLDVFTNIRDDELEHVKTMVACQESTIAKDIAASSSGSAPRR

>pti:PHATRDRAFT_44482 K00387 sulfite oxidase [EC:1.8.3.1] | (RefSeq) hypothetical protein (A)

MLSKKVLSSFQKSSVGACVLSGTRRVSTAHVRCVSVAALSHFAGNDNASLSSKCSLMNVAAAAAAATATI
LTWAGATSLCDSNAKPMSTEDSHLTPSEVGKEDFEEFQASHDINSMPVYSLEEIAEKNGENGNPIWMSYGG
VVYDVTDFIPNHPGGSEKILTAAGSAIEPFWYLYRQHFASDLPMRLMEHMAIGRLSEEDQERIEEQMATLEE
TDPYAKEPYRHRALLVHSDTPMNAECPTRFLTQNFLTPASIFYIRHHHPVPFLSEKQVNDFRLKVDLTAYGK
GVVLYSVDELRKMKKVEITATLQCSGNRRSGFNQFQRTSGTPWGQGAISTAKFGGVRLTDLLKASGLKDPI

EAEEKLGLEHVRFHSLDGMSASIGMEKAMNPYGDCIVAYEMNDEPIPRDHGFPLRIIVPGYAAVRNVKWL
EKIELAKTEAEGPWQRGLNYKTLPPNMTNAKNVDLNKMPSMTEVSLFSGITQVEKPEMKEGMKAGDKITV
KATGWAWAGGGRNIVRVDVTGDNGASWATAILKEGSEQRFGRAWAWTFWECDVPAIVQEDGNVHLAS
KAVDLAFNAQPEDANHTWNVRGLGNNSWYRTKIRILE

>gtt:GUITHDRAFT_108738 K00387 sulfite oxidase [EC:1.8.3.1] | (RefSeq) sulfite oxidase (A)

MTTWRRVNDEEQWQGIKQAVALGLASLFVGAAWMVSSRETSCEAKVDDDEDKFTPEERKALPAPGQVN
NLKLYTKAEVAQHISREAGGIWVTYKDGVYDITEFIESHPGGASKILLAAGKAIDPYWNIFQQHFRTGFPLQ
LLESMRVGSLAPGEYVEEKQADPYAVDPIRDERLILHNSAPCNAEIPEHYIMESYLTPNELWFVRHHNPVPII
DPNNYTLTIKGKLQEKFPKHEVDVTIQCSGNRRSHFDGVKKAQGIPWNMGGVSTARFGGARLKDVLEYCG
VKDPEKNGIHHVQFISQDEMLASIPIEKAFSYSGDVLLAYEMNGEEIPTDHGYPVRAVVPGYVGVRNVKW
VKEVFVSEQEAEGPWQRGVAYKGFASNITDLQHLPTHVIERAAPVQEPPVTSLIVHPANNAKVHSQTLEVR
REDVRVRVTGEQLKGWAYSGGGRGIVRVEVSIDGGKSWHTAELKEGSEQKLTRAWAWTFWSANVEVPK
ELQGKSSEIMCRATDASYNSQPEHASSIWNVRGLCNTAWHRKTVHFD

Probes for ROS Scavenging enzymes

> Chlorella variabilis GL433837 Fe SOD

MAFTLPPLPYAMDALESKGMSKQTFEFHYGKHHAAYLNNLNGQVAGKELANAASVHEVMLATWNGGKP
GPEFNNAAQVINHTFFWESMSPSGGGKPGGKVAEAIEKDLGGYDKFVEAFKAAGATQFGSGWAWLSVGK
EGKLEVSKTANAENPWVHGATPILTLDVWEHAYYLDVQNRRPDFISNFISNLIDWQRVEQRYLEATK

>Phaeodactylum tricornutum Fe Sod

AYSVPDLAYPFEALEPYIDTPTMKIHHDKHHGTYVANINKATEGKDEVPILDLMENAIEAGPAYRNSGGGH
YNHAFFWDEMAPPDQAKNTKPSAQLVDLINASFGSMDEMKSKFEALAAPGATFGSGWVWVCVNQKGDE
LKLVNTPNQDNPLMKGVADEIMFPILGLDVWEHAYYLKYQNRRPEYVSNFWNVVNWDKVSENCAYVVE
KHVGVSVRG

>Ostreococcus lucimarinus CCE9901 Mn-Superoxide dismutase

MLSRAVTTSARRCRALASSRAPTRAFVSAKLPDLDYDFSALEPVICAEIMEIHHQKHHNTYVTNFNIAQEKY
AEAEAKGDYAGMIAMQPAIKFNGGGHVNHALFWKCLTPPKDYALPEGELLKMIERDFGSLNAMQDKFTA
ATVAVQGSGWGWLGYDKANKKLAVTTTANQDVCLSTGLTPILGVDTWEHAYYLQYKNLRPDYVKNLW
KIINWKNVGENLKSAM

>Thalassiosira pseudonana Mn Sod

ETGSNRRQILQKGAAIATTIATPLVSNAYSVPDLNYPFEALEPYIDAPTMKIHHDKHHATYVANINKATEGK
DEVDILELQLNALEAGPAVRNNGGGHYNHAFFWDEMAPPDEAKKTKPSADLEAMINKSFGSLDEMKAAF
EARAAPGALFGSGWVWICVNQKGDELKLVGTPNQDNPLMKGVADEVMFPILGLDVWEHAYYLKYQNRR
PEYVSNWWNVVNWDKVSENFAYVVEKKAGVPVRG

>Ostreococcus Tauri RCC1115 Cu/Zn SOD

MSTGPHFNPNKMDHGAPTDAVRHAGDLGNVDASATGCDFTIEDSQIPLSGANSIIGRAFVIHELEDDLGKG
DSSEIGTQGKTSKTTGNAGARLACGVIALTNA

>Fragilariopsis cylindrus Cu/Zn SOD - sod1

MATCVCVFISEGSSGVTGSISLVQNQEDSPTVIEGQLRGLTPNQRHGISVCTYGDARDSSSSCGPIFNPFGKT
HGSPSDDPALRMEGDLGNITADASGNATIKVDESNIKIYGPHSVIGRSIVICAGADDEGRGGHENSLSTGNA
GPRVAYGVIGLSNPTSA

>XP_022838337.1 Superoxide dismutase, Nickel-type [Ostreococcus tauri]

MQIFARTVRGRTLVVRDARTVGDATAALRARGETFDYVTNARGRVLRSDDVVEGDSTVHARVRVLGGHC
QVPCGIFDDPAMVAQLREMSATIRKAMTQINELSATNTPLAINQMTRWVMTKEEHCAKIITMIGEYCLCQR
VKAAEMSPEDYVDALKIHHLVMQNAMKCKQNVDTDFCCHLDHSLDDLAKMYTKA

>Ostreococcus tauri version 140606 Ascorbate peroxidase

MSAARRVDAVANHLHAAASVNAVDAAAYASDLRAMKMDIERFLDESNANPIMVRLAWHDAGTYDASK
AHMPWPRAQGANGSIRHESELAHGANAGLVKAIGYLRPLKEKYARVSWADAIQLAGATAIEHAGGPRIPM
RYGRADAEVGAMEGNLPDAEAPFGDGASDAATHLRNVFGRMGFNDREIVALSGAHTIGRAFKERSGTTN
HGYGAKNGTKFTGCPYMNARADGKEGSIGMPGGASWTRRWLAFDNSYFHREKLTDEKDLIWLSTDDAL
VTDPGFAPHFKRYAHDQNAFFYDFSAAFAKLSELGSRFVVGASGIVL

>Fragilariopsis cylindrus APX

MKSSLAAISFIFAATTTTVNAFVNPSTTRSYSVFQQNISNNKNNININIMTAATSINQTPKTVALAAAAAVSDTKV
SANEYKEALLAARDDIDILLAENACGPLMVRLAWHDAGNYDKNLASEKWPLAGGATGSIRFAPEINHGAN
AGLINGVKLIQTHIKEKHPLISYADLYQMASSRAIEYTGGGPSLGIRYGRQDVDSPDGCQKEGNLPDGEADP
DTGNYGGTSGTASTEDKTPGGHLRKVFYRMGMNDEEIVALSGAHSLGRAYHDRSGLGAEQTKFTDGSTT
QKFANGKVAPFHAGGSSWTEQFFVFDNSYFIVLNDDKSDPELLKMSSDKAVFKDDDFRPYAEKFRDNKES
FFESYVKAHNKLSELGSKFVYDTPITLD

>Bathycoccus prasinos monodehydroascorbate reductase

MAQRRVVIVGGGNSAGYLVRALVGAPSSSSSLSSPSSSSVTIVSEENVLPYERPALSKAFLNEQSPARLPGFH
TCVGGGGERQTEEWYKEKEVETKLGTKITKCDYEKKRVETASGEIIEYDALVIATGVSAHKGSFIEGFDGK
MCKVLRSHEDALEVVKAMDAKPKHPVVVGGGYIGLEVAAGMCARGLKPTVVLLESNIMARLFTKEIAAH
YEQLYESKGATFIKNASVKKINDGKSVILNDGRELDADLVVLGVGSDVRPNVEPFCDSSSGGLLEKGKDGG
IKVNGKFETSQKDVYAIGDVCSFPVRLTGPNENEEHYRMEHVKHARASAAHCARTLIGEKDVPDYKYEPFF
YSRVFEQPNSDRPVSWQFYGFGGHAAMETGKVSAVGPIGDFKPQLVSFWIETSTKKCIGCFLESGGSIETQI
AKDLGEKNPVVDVDALAKSATVAEAMSVCAEALKKN

>Cyanidioschyzon merolae MDHAR

MLEVHRLVTRSHLSSFVCFLEKLGNHQRLFGKGVSAPKVKGSTRLSSVCKRCLVMSATSVKSYEYVILGGG
NAAGYAARQFVEKHGLSGHKLAVISRESVAPYERPALSKAYLTANPPTRLPAFHTCVAGGGAPQTPDWYA
KNGIDLLLSTEIVDCDLNSKCLTAKDGSKYGYGKLLIATGSDALHLDELGMQGAHLGGIHYLREIAEADKL
YEAMKACAGKHAVVVGGGYIGLECTAALVINGVRVTMVFPEPHVMARLFTPEIAAHYERIYAQKGVNFIK
GTVVDSFADENGSGQVKYVRLKNGPVLEADLVVVGVGAKPRTTLLEGALAMEARGIKVDGHLRTSHADV
FGAGDVITFPLKMYGNRMARVEHVGHARQSAMHAVDVMMGATTEPYDYLPFFYSRVFHLSWKFWGDTP
AQAKTIVVGEMNPKLVAVWIDQDGHVVGTFIESGTEHDENKLKELARTRPKANVARLEEAAAAANDVDGF
LNAL

>hypothetical protein DHAR Chlorella variabilis (K21888 ec.[EC:1.8.5.1 2.5.1.18])(higher scores on NCBI blast to DHAR)

MATGGGSQGPEFEVHVLGHPKGGPEGHEGQLGACPFSHRVLLLLEERELPYTVDFVDVARKPDWVTETNP
EGTLPILRDCASGQLLHDSDAISDFLEDKYGGGDGKRSLRKLGDCPQPAPQLWPKFLAYLGAEAGSQEEAA
ARRELEEQLQASPALLP

>Ostreococcus lucimarinus CCE9901 glutathione reductase

MLVAKLSSQGFNLVRFQKRTALRVVASAKNTEGARVMRTAAVRGASSEHGFDYDIFVIGGGSGGVRASR
MASSAGAKVGLCEMPYDPISSDRTGGLGGTCVIRGCVPKKLFVFGSGFSADFEDASGFGWVLSEPKLDWK
RLLDAKLKETERLNGIYERLLDGSGVTSYVGAGKLLDNHTVEITGQEGSKESVTARDILIATGGRAYVPDIP
GAELGITSDEALNLTELPKKMVIVGSGYIAVEFAGIFAGLGVEVDLVYRQALPLRGFDDDIRSTVYSNLKER
GINQISSCQLVSLDKQSDGRLLLRTSTEELETDVVIFATGRIPNTTRPKLGLESVGVELSATGAIKVDEYSRTT
VSNIWAVGDVTDRVNLTPVALMEGMAFVDTVVRGNPTKPDYENIPCAVFSQPPVATVGLSENDAIMRGVR

CDVFMSSFTPMKYSLSGRKEKALMKLVVDSVSQRVLGVHMVGPDAAEILQGFATALKCGATKQHFDQTV
GIHPSSAEEFVTMRSLTRTVGGE

>Fragilariopsis cylindrus GR

MSHVQSRKAKAIFTADLFTIFLNSPRSSFLFQNYTQRRSHNYYILVLRTNYLITIIYIMSEQSYDFDLVVIGGG
SGGLACAKRSAQNGKKVAVIERARLGGTCVNVGCVPKKIMFLTSTMAEQMKHDATQYGFEQPNVRLNYP
LLKKRRDAYIVKLNGIYERGLNNAGVGKIIGDATFAGAHTLSVTNDGNTQSVTADKILIAVGGRPNMTPIPG
IEHCISSDGFFEMEELPTKAVVVGAGYIAVELAGVLNGLGVDTHLVVRKHKALRTFDEDISDFLDSEMVRQ
GITIHRNTGGLSKVVKQDDGKMSTYMVAEDKESISDADIVLYATGRLPNTETLNLDKVGVKLVEGKTYIK
ADDFQNTTAESIYALGDVCGKVELTPMAIAAGRRLSDRIFLDKADSRTSYELVPTVVFSHPTIGTIGLTESEA
IDKYGKDNLKVYKSKFPNLYYGIFQMESEDKPKTLMKLVCAGKEELVVGLHICGMSADEMLQGFGVAMK
MGATKADFDSSIAIHPTGSEELVTMGVWGTSSQETGAKVSPLMGSSPPEPTI

>Coccomyxa subellipsoidea C-169 catalase

MDPQKYLPSSHHDSPYWTTNSGAPVWNNNSSLTVGQRGPILLEDYHLVEKLAQFDRERIPERVVHARGAS
AKGFFEVTHDISQLTCADCLRSPGVQTPVIVRFSTVIHERGSPETLRDPRGFAVKFYTREGNWDLVGNNFPV
FFIRDGIKFPDMVHALKPNPKNHLQEDWRIADFFSHIPESMHMFTFLQDDIGIPANYRHMEGFGVHTYTLIN
KEGRVTYVKFHWQPTCGVKNLLEDEAVVVGGSNHSHATQDLYDSIAAGDYPEWKLLIQTMDPKDEDKFD
FDPLDVTKIWPEHLFPLQPVGRMVLNKNPDNFFNENEQLAFCPSLVVPGIGYSDDKLLQTRIFSYADTQRHR
LGPNYLLLPANAPKGPHHNNHHDGFMNFTHRDEEVNYFPSRFDPVRHAERHPINNTFVSGQREKRIIQKEN
NFKQPGDRFRSFDPARRERFVNRIAGMLSDPKCTQEVRRVWIGYLSQCDASLGQKVAAKLQSNGAF

>Phaeodactylum tricornutum catalase

MSDQTSSRDAASNQLDAYASQRYVVSPAIELLKASNGAPVDSLTASMTAGPRGPIVLQDFTLLDHMARFD
RERIPERVVHAKGAGAFGVFQVTSPEPIRSVCKAQVFQSMEPTPVAVRFSTVGGETGSADTARDPRGFAVK
FYTTEGNWDLVGNNTPIFFIRDPMLFPSFIHTQKRNPATHLADPDAFWDFIGLRPETTHQVTFLFSDRGTPDG
YRHMNGYGSHTFKNVNSNGEAVYVKYHWKTDQGVANLDAEHAARLAASDPDYATRDLYNAIATGNYPS
WTLYVQIMTYAEAAAVDNPFDLTKVWPHSRFPLHEVGRMTLNRNPKDYFAEVEQLAFAPSHLVPGIEPSP
DKMLQARLFSYPDTHRHRLGTNYQAIPVNAPRNISAAQQHNYQRDGPMQVTENGAGAPNYFPNSFGGVQ
PPPATAHGPELAWHADTVSGQVVRIDTGDEDNVSQCRDFYRNVLDQAARARLTDNLAAHLCRAQPFLRA
RAIHNFTQVDSTFGAQLKAAVAQKVMHTPPPSQSRRRPAKLNPPRIVPPPTASRGLCPAGYGNQGSPAHGY
ASKL

>Phaeodactylum tricornutum CCAP 1055/1 catalase-peroxidase

MGSDSKCPFAPKMNKAASANSYWWPDNINLKILNQQGANNPDPSFNYKEAFRELDVEMVKRDVNKMLT
TSQDWWPADWGHYGPFMIRMAWHAAGTYRISDGRGGANTANQRFAPLNSWPDNANLDKARRLMWPVK
QKYGRKLSWGDLMMLTGNQALEIMGLKTIGFAFGREDIYSPEDDVYWGPEKEMLSNDRFDENGDIKRPLG
ASEMGLIYVNPEGHDNEPNPTKSAHDIRQTFRNMAMDDYETVALIAGGHTFGKTHGAAPVSHQGPEPEGA
SIEHQQLGYLSDYGTGKGKDTTTSGLEGAWTETPIQWDMNYFKNLFEYEWEVHKGPGGRHQWRPTDKST
FEMVPDAHEKGKKNPPMMFTTDISLKIDPIYGPISRHFYHHPDEFSAAFAKAWYKLLHRDMGPVSRCLGSD
VPEPQLWQDPIPSLDHELIDDEDVAKLKKQILGSTGIAGKILGSSGPCVSELVKVAWGSACTYRGTDHRGG
ANGARIRLAPQNTWKVNDPEELKRVLEHLEQIQLDFNEQQKGSNKRVSLADLIVLGGCAAIEYAAKNAGN
DINIPFSPGRTDASSEQTVAESFDALEPSADGFRNYLKEGQSAKPEELLLNHAHLLTLTSPEMTVLLG
GLRVLKANTGNSEMGVFTKNPETLTNDFFVNLLDINTTWSSVEQDKNLFDGLEYGTGKLNWKASRFDLIF
GSNSELRAIAEYYGSDDSNEVFLKDFVKAWTKVMELDRFDLK

>Micromonas commoda glutathione peroxidase

MVMGIFHALFGSSPKTSVASFFDFKDVKDIDGHPHDFTQYRGKVVIVSNTRCHYDEFAELKRRFGDALVV
MGFPCNQFGMQEPGSNDSIRDWCARRGFIPNVGVLMEKCKVNGSGSSPVFDFLKVQSGTGGVMWNFCKY
LVAPDGVTVHKFGPEKDPRHLIPKIEELIAQARRAEE

>Fragilariopsis cylindrus GPX

ELQKKYGSEGFSVLAFPIKDFSQELGSNEEIISFMDENFPQVDFPLFSLSSLKENPVYQKLHKQKPDNHIKWN
FYKFLIDWNGQVVEFYDKKVSPMQISDQIEQLL

>OT_ostta03g02825:K03564_ peroxiredoxin Q

MSYSCLSVVASTRAVVASTRARTGRARRASARVEASGDDAVKVIDRRAVLRGALSLAALDVLAPSRARA
VNIGDKAPDFTLRGTKGASVHLGDVLNEQKFTVVYFYNQDGSPGCSVEAQRFEAAIPEFAKREARVLGISM
DSLDKHEQFCADKGLKSFTLLSDGDGSVSESYGADLKIPIFGRFSDRQTFLVDGNGTIINHWLERDQSMASV
KTTAHVEQILNAIDAA

>Fragilariopsis cylindrus PRX Q

MKFISAIVSAVCLVNAVDAFAPPASFSSSSASAASAASSALHLAVGEVAPDFSLQDQNGKTIKRSSIKKPLVI
YFYPSDSSPGCTKQAQSFNDRITSIRKTYGADVVGISGQDVESKQKFAVEEGLTFSILADADDAVRKEFNVP
KELFGLFPGRVTYVLDKAGVCQLVYKELSKAESHVMKAEETLEEMKATNTGGGAGNPFAALFNK

>Monoraphidium neglectum_K20011 (peroxiredoxin 3)

MARIGKKAPAFKGQAVLPSGEIAEISLDDYLNKGKYIVLFFYPLDFTFVCPTEIVAFSDRIKEFEEINTTVIGA
SVDSHFSHLAWVNTPRKAGGLGGISYPLLADLTKQISKDYEVLIEDGPDAGVALR

>Chlorella variabilis_K11187 (peroxiredoxin 5, atypical 2-Cys peroxiredoxin)

MWVAGGWAGAQPAAAWCIVQVGDSLPDIKLDQLEDGEIKQVSLKQLFSNKKGILFGVPGAFTPGCSKTHL
PGYVADREKLREAGAEVVVCVSVNDPFVVGAWGEAHNAGGKIVMLADTRVRGLGASGMNDVVAWRSC
LPTRSHGRCAAFSAVVEDGVIKSLNLEEGGGMTCSLSNQILSQLKQ

>Fragilariopsis cylindrus PRX5

MNTILRLCLLFTSFSAVHSFFGLQLSSSSSSSLTNLSLSTPATDNNMVVEEVKVGDTVPSITLQEGLPEFGKK
DVNISELIAGKKAIIFGVPGAFTPGCSKSHVPSFIHAKEELKEKGIDIIICIATNDLYVMKAWGEHSGGTDAGI
VFLSDGSAELTQALGLVMETPMMPRTKRFTLIAENGIVTQYFSSAEESSNTWAPAVLAKL

>Bathycoccus_K11188(peroxiredoxin 6, 1-Cys peroxiredoxin)

MPLNLGDTVPDFSCDSSVGQIHYYDHVGDEHWSILCSHPSDFTPVCSTELGTLAKLLPQFERRNCKVLALSC
DNAESHRKWIKDIDASGYCGKTTSTVSYPILADEERALAVKFGMLDPEEKDEKGQPLTCRAVFIVDDHKKL
RATILYPATTGRNFYEILRVVDSLQLTDEYPVATPANWERGEKVCVTPSTPDEVAQVVLGDFSVVKVPSGK
KYLRLSKDPGYKTPKVLKRGMVETILGTEYGAKLLPTLGRLVVAFALGGFSSSFASSKKKEKPVHTTPQTS
GWKKR

>Thalassiosira pseudonana PRX6

FPDIQGETQETTGFSLYNYLGDSWCCFLSHPADFTPVCTTELGAAQSLVEEFAIRDVKLCGFSCDDSKRHKD
WISDIDAATGHRISFPLFCDPSRKYAIELGMLDPTLKDDEGMPLTVRAVFILNSAKEITLTMTYPACVGRNF
DEILRAVDALQRAEKFGVVTPANWQPGDKTIVSLDLDDDAAMRKFGKGYSTLDLPSEQVRHLHKHYLRY
TDDP

>OT_ostta03g02825: K03386_ peroxiredoxin (alkyl hydroperoxide reductase subunit C) [EC:1.11.1.15]

MFRRAARAVAQRACAVATHTVSRTTLPCAERAVVANSNAMTQRARNLVHAQRFTRAYADDATTRVRYP
RSEVFVGEQAPGFDAPAVIDGELGRINLKEYAQGGYCVVFFYPLDFTFVCPTEITAFNDRASEFEELGAKVI
AVSTDSEYSHLAWTMTERESGGLGPMRIPLVADRTKEISAKYGVLLEDTGIALRGLFIIDDEGVVQQITVNS
LPVGRSVDETLRLLRAIQYTKEHGEVCPAGWTPGDPTMVGDPEKSKEYFEAHAGKTPASSSSSSAXXXXX
XXMDADVVIIPPFGLQKGTKTNGEMAAMVFRETQAAQQANTQPATQSERCVHNDGKAWRCPASRVDDT
PFCSKHGPVKYATSVRVRPVSFTTQQGLEVTYAGPPSACVIRSVASTPIASLDLLSLKDPENFEAHAWKIESQ
LKSCDGLIRRDGPCGRFRENAVVLERGGVWVPYETYEARLITLLPGTPPGSSVASETVLNQCIEDINRINASR
SAANEGENDDSNEDPTASDGTNENSAPIDGSPGDDPTVKMPTGAREVRLRLAELHRQLNTVKREISGLKET
GVEHAEALKREGGEDESEYAAFEQSINRALQLT

>Thalassiosira pseudonana peroxiredoxin (alkyl hydroperoxide reductase subunit C)

MVTFPQIGKRAPNFVTVGVFKKRLGRIRLSDYRGKKYVLLFFYPANFTPVSPTELINLSDRISEFRKLSTQILA
VSIDSPFSHLQSLLLSRKEGGLANLNYPLISDLSQTITKDYKVLTEEGLGLPGVFIIDKEGIIQYYTVNNLLCSR
SVNELLRILESIQYVKKNPGQACPENWHPSSLIGRQQYDQILYSHPLKSKLYFRDLYSSKKN

>PRX1 (K13279)Nannochloropsis gaditana

TATRPGVQGSEGLQLHFRQIISPACETSRRVRKWQIRSKFMIKDIFFPFFCTLALSFLSCPSIPVTLAQSVSGT
MATNKPVPMIGKPAPDIKAEAVMPDGSFKELSLKQYRGRYVILVMYPLCPSELIAFSDRIQEFHDLNADVV
GLSVDSKYSHLAWSRSPRKLPATTVC

>Ostreococcus lucimarinus_cytochrome c peroxidase [EC:1.11.1.5]

DADFGPTLVRLAWHSSGTYDRMGKTGGSGGGTIRFKEELAHGGNAGLDKAIAKLEPIKKRHPDVSWADLI
AFVGVVAIEEMGGPKLKFSYGRVDEMDPEAVTPDGRLPDADKGDGPGPKTRQGLRDVFYRMGFDDREIV
ALSGAHALGRCHADASGYVGPWSGTPLLFNNSYFVLLKGLKWEPNPDAKKFQYKDPSGNLMMLPSDIALI
EDADFKKYVDVYAKSQKVFFEDFAAAFEKLETLG

>Fragilariopsis cylindrus CCP

MIFNYARFANRLAAPAVFGSTLALYSLQDVHAKEATVDMNKVRDAIMKVVEDDAEKRDDGTSMAGTLIR
LAWHCSGTYKADDNSGGSNGARMRFSPEAKYGNNAGLDRIRATLEPIKEKFPGMSYSDLYTYAGVVAVE
EAGGPKIPYKTGRIDMVDGSKSDPNDRLPNADYGGRDKNVESIRKIFSRMGFNDNEFVALMGAHAMGRCH
TQDSGFSGPWTFAETTFSNEYFRLLLEERWSPKIEHEGKPWKGPDQFEDSTGKLMMLPVDMMLIMEPAFK
KWVDVYAKDEDKFFTDFASAFAKLLALGVPAAAIPSIGKPWYQIW

Appendix 2

Dropbox link containing BLAST+ output

https://www.dropbox.com/sh/ab5oam9grmbr9t4/AACuKRGsMXxY2lELgXluhQxxa?dl=0

Dropbox link containing all the code

https://www.dropbox.com/s/jla23g9jrmsis84/naaman_thesis.Rmd?dl=0